Vglut2-based glutamatergic signaling in central noradrenergic neurons is dispensable for normal breathing and chemosensory reflexes

Author names and affiliations

Yuan Chang[1], Savannah Lusk[2], Russell Ray[1,2,3,4]

[1]Department of Molecular Physiology and Biophysics, Baylor College of Medicine, Houston TX

[2]Department of Neuroscience, Baylor College of Medicine, Houston TX

[3]McNair Medical Institute, Houston TX

[4]Corresponding author, russell.ray@bcm.edu

Abstract

Central noradrenergic (NA) neurons are key constituents of the respiratory homeostatic network. NA dysfunction is implicated in several developmental respiratory disorders including Central Congenital Hyperventilation Syndrome (CCHS), Sudden Infant Death Syndrome (SIDS) and Rett Syndrome. The current unchallenged paradigm in the field, supported by multiple studies, is that glutamate co-transmission in subsets of central NA neurons plays a role in breathing control. If true, NA-glutamate co-transmission may also be mechanistically important in respiratory disorders. However, the requirement of NA derived glutamate in breathing has not been directly tested and the extent of glutamate co-transmission in the central NA system remains uncharacterized. Therefore, we fully characterized the cumulative fate maps and acute adult expression patterns of all three Vesicular Glutamate Transporters (Vglut1, Vglut2, and Vglut3) in NA neurons, identifying a novel dynamic expression pattern for Vglut2 and an undescribed co-expression domain for Vglut3 in the NA system. Our functional studies showed that loss of Vglut2 throughout the NA system failed to alter breathing or metabolism under room air, hypercapnia, or hypoxia in unrestrained and conscious mice, which demonstrates that Vglut2-based glutamatergic signaling within the central NA system is not required for normal baseline breathing and hypercapnic, hypoxic chemosensory reflexes. These outcomes challenge the current understanding of central NA neurons in the control of breathing and suggests that

glutamate may be not a critical target to understand NA neuron dysfunction in respiratory diseases.

Introduction

Breathing is a vital and life-sustaining function supporting homeostatic processes, most critically maintaining blood pH/CO_2 and O_2 levels within a narrow physiological range. Respiratory homeostasis is mediated by neuron-modulated lung ventilation adjustments in response to physiological deviations resulting in high pCO_2 or low pO_2 blood and tissue levels, known as the hypercapnic and hypoxic reflexes respectively (Del Negro et al., 2018; Dick et al., 2018). These reflexes are part of a complex brainstem neural network that integrates a multitude of information streams across the central and peripheral nervous systems to regulate respiratory output. Within this brainstem network, central noradrenergic (NA) neurons are known to be an important component that plays a variety of roles in modulating breathing. Furthermore, various perturbations across the central NA system have been implicated in several developmental disorders with respiratory and chemosensory features such as Central Congenital Hyperventilation Syndrome (CCHS), Sudden Infant Death Syndrome (SIDS) and Rett Syndrome (Beltrán-Castillo et al., 2017; Feldman et al., 2013; Gauda et al., 2007; Viemari, 2008). Thus, understanding how central NA neurons modulate respiratory chemoreflexes or chemosensory breathing is critically important for the development of new diagnostic and therapeutic interventions to address respiratory pathophysiology.

Central noradrenergic neurons are commonly thought to exert their effect on breathing through their primary neurotransmitter noradrenaline and adrenaline. However, in addition to noradrenaline, several studies suggest that glutamate is co-transmitted in subsets of central NA neurons. Vesicular glutamate transporter 2 (Vglut2), a gene marker of glutamatergic signaling, has been shown to be co-expressed in subsets of central NA neurons including, C1/A1, C2/A2, A5, and LC in adult rats and mice (DePuy et al., 2013; Souza et al., 2022a; Stornetta et al., 2002a, 2002b; Yang et al., 2021), though NA specific expression of related Vglut1 and Vglut3 transporters remains unknown. Additionally, it has been well documented that central NA

58 neurons co-expressing Vglut2 innervate key respiratory centers, such as preBötzinger complex
59 and parafacial region (pFRG), as well as many other autonomic brainstem and forebrain centers
60 that could indirectly drive a change in breathing if perturbed, i.e., cardio-vascular function, the
61 intermediolateral nucleus (IML)-sympathetic system and metabolism (Supplemental table 1).
62 Thus, it has currently become a dominant paradigm in the field of respiratory physiology that NA-
63 based glutamate release is a critical form of neurotransmission in the control of breathing. This
64 paradigm is supported by multiple papers. Abbott et al. (2014) showed that Vglut2 is required for
65 an increase in respiratory rate when anterior C1 neurons are unilaterally opto-genetically
66 stimulated. Malheiros-Lima et al. (2020) showed that Vglut2-expressing C1 neurons project to
67 the pFRG region, and hypoxic breathing was blunted after blockade of ionotropic glutamatergic
68 receptors at the pFRG site in anesthetized rats, together supporting a role for anterior C1 neurons
69 releasing glutamate at the pFRG site in turn to regulate breathing under hypoxia. Similarly,
70 Malheiros-Lima et al. (2022) and Malheiros-Lima et al. (2018) showed that Vglut2-expressing C1
71 neurons project to the NA A5 region and the preBötzinger complex respectively, and again the
72 blockade of ionotropic glutamatergic receptors at the A5 region or preBötzinger complex reduced
73 the increase in phrenic nerve activities or in respiratory frequency elicited by optogenetic
74 stimulation of C1 cells in an anesthetized preparation. In addition, Guyenet et al. (2013) and
75 others speculate that the apparent lack of plasmalemmal monoamine transporter in C1 fibers
76 indicates reduced or absent noradrenergic or adrenergic signaling due a lack of re-uptake and
77 neurotransmitter pool depletion (Comer et al., 1998; Lorang et al., 1994). Cumulatively, the
78 studies argue for glutamate as the predominant functional neurotransmitter for C1 NA neurons
79 in the breathing neural network. To our knowledge, this dominant perspective has not been
80 otherwise previously challenged. Although these studies are informative, the evidence
81 supporting the role of NA-based Vglut2 signaling in respiratory control are either indirect and
82 circumstantial or cannot be seen as physiological given experimental limitations, such as the focal
83 nature of opto-genetic stimulation. Thus, it is not yet clear what the requirement is for NA-based
84 glutamatergic signaling in homeostatic breathing in the awake and unrestrained animal and how
85 that might inform upon disease.
86

87 To better understand the role of NA-based glutamatergic signaling in breathing, we sought to
88 both fully characterize the molecular profiles of the central noradrenergic system with respect to
89 glutamate co-expression and to determine the requirement of Vglut2-based glutamatergic
90 release in respiratory control under physiological chemosensory challenges in awake and
91 unrestrained mice. We first fully characterized the recombinase-based cumulative fate maps for
92 Vglut1, Vglut2 and Vglut3 expression and compared those maps to their real time expression
93 profiles in central NA neurons by RNA *in situ* hybridization in adult mice. We found a novel
94 dynamic expression pattern for Vglut2 and an entirely undescribed co-expression domain for
95 Vglut3 in the central NA system. Secondly, to determine if Vglut2-based glutamatergic signaling
96 in NA neurons is required for respiratory homeostasis, we conditionally ablated Vglut2 in all NA
97 neurons and tested respiratory, chemosensory, and metabolic function in unrestrained and
98 conscious mice. Using the same genetic model in prior studies (Abbott et al., 2014), conditional
99 deletion of Vglut2 in NA neurons did not significantly impact breathing under room air,
100 hypercapnic, or hypoxic conditions. These results demonstrate, for the first time, that NA Vglut2-
101 based glutamatergic signaling is dispensable for respiratory control, which challenges the
102 prevalent perspective on the role of C1 and other Vglut2 expressing NA neurons in respiratory
103 homeostasis and suggests that glutamate may not be a critical target to understand NA neuron
104 dysfunction in respiratory diseases.
105
106 **Results**
107 **Cumulative fate maps of central noradrenergic neurons co-expressing Vglut1, Vglut2 and**
108 **Vglut3**
109 To fully characterize the expression profiles of all three glutamate markers Vglut1, Vglut2 and
110 Vglut3 in central noradrenergic neurons, we first used an intersectional genetic strategy (Figure
111 1A). We bred three Cre drivers *Vglut1-Cre/+, Vglut2-Cre/+ and Vglut3-Cre/+* to *DBH-p2a-Flpo/+*
112 (targeting noradrenergic neurons) mice respectively. The three compound lines of *Vglut1-Cre/+;*
113 *DBH-p2a-Flpo/+, Vglut2-Cre/+; DBH-p2a-Flpo/+, and Vglut3-Cre/+; DBH-p2a-Flpo/+* were then
114 crossed with the *RC::F_TdTomato_P_GFP (RC::FLTG)* intersectional reporter mice which express
115 tdTomato in cells expressing only flippase (Flpo) while expressing eGFP in cells co-expressing both

116 Flpo and Cre recombinases. Thus, in each of the three intersectional reporter crosses [e.g. 1)
117 *Vglut1-Cre/+; DBH-p2a-Flpo/+; RC::FLTG/+,* 2) *Vglut2-Cre/+; DBH-p2a-Flpo/+; RC::FLTG/+, and* 3)
118 *Vglut3-Cre/+; DBH-p2a-Flpo/+; RC::FLTG/+*], NA neurons without any Vglut1/2/3 expression are
119 labelled by red fluorescent protein (tdTomato) while NA neurons co-expressing either Vglut1,
120 Vglut2, or Vglut3 are labeled by green fluorescent protein (eGFP). By using this method, we
121 characterized and quantified the expression profiles of all three vesicular glutamate transporters
122 Vglut1, Vglut2 and Vglut3 across every NA nucleus in adult mice including A7, Locus Coeruleus
123 (LC), sub CD/CV, A5, and throughout the anterior - posterior dimension of C1/A1, C2/A2 (Figure
124 1B-D). *Vglut1-Cre* was not co-expressed in any central NA nuclei in adult mice. However, *Vglut2-*
125 *Cre* and *Vglut3-Cre* both showed co-expression in central NA neurons. *Vglut3-Cre*-expressing NA
126 neurons are restricted to posterior C2/A2 and posterior C1/A1, and the majority is in posterior
127 C2/A2 where 26.9 $\pm$ 3.16% NA neurons are *Vglut3-Cre*$^+$. In posterior C1/A1, only 1.26 $\pm$ 0.559%
128 NA neurons are *Vglut3-Cre*$^+$. Surprisingly, 84.6 $\pm$ 3.75% NA neurons in total have *Vglut2-Cre* co-
129 expression and each NA nucleus was predominantly labelled by *Vglut2-Cre* expression. The
130 percentage of *Vglut2-Cre*$^+$ NA neurons in A7, LC, A5, sub CD/CV, anterior and posterior part of
131 C1/A1, anterior and posterior part of C2/A2 is 69.8 $\pm$ 8.29%, 80.5 $\pm$ 3.78%, 84.8 $\pm$ 11.3%, 51.5 $\pm$
132 2.61%, 99.0 $\pm$ 0.681%, 95.7 $\pm$ 2.40%, 96.1 $\pm$ 1.98%, 97.8 $\pm$ 0.771%, respectively (Mean $\pm$ SEM).
133 The presence of *Vglut2-Cre* co-expression in anterior NA groups was unexpected as previous *in*
134 *situ* data in adult rats found Vglut2$^+$ NA neurons only in the posterior C2/A2 and C1/A1 (DePuy et
135 al., 2013; Stornetta et al., 2002a, 2002b). Notably, however, the Vglut2 co-expression in the LC
136 region agrees with Yang et al. (2021) which also showed that a high percentage of LC NA neurons
137 are Vglut2$^+$ by using another intersectional strategy in mice, *TH-Flp; vGluT2-Cre; Ai65.* The
138 differences in our and other fate maps compared to *in situ* hybridization may either reflect early
139 gene expression that is down regulated in the adult or may reflect low levels of expression not
140 detectable by *in situ* hybridization but that are nonetheless sufficient to effect recombination in
141 the intersectional genetic strategy.
142
143 **Real time mRNA expression patterns of Vglut1, Vglut2 and Vglut3 in central noradrenergic**
144 **neurons in adult mice**

145 DePuy et al. (2013), Stornetta et al. (2002a) and Stornetta et al. (2002b) showed that Vglut2 co-
146 expression is only located in the C2/A2 and C1/A1 region in the adult rat but not in anterior NA
147 nuclei in the brainstem by *in situ* hybridization. To verify if the real time NA-based Vglut2
148 expression pattern in adult mice is the same as in adult rats and to further characterize the
149 expression patterns of the other two vesicular glutamate transporters (Vglut1 and Vglut3) in
150 adult mice, we performed fluorescent RNA *in situ* hybridization experiments. We co-stained
151 Vglut1, Vglut2, Vglut3 with DBH respectively in brain tissue of adult mice and characterized the
152 colocalization of Vglut1/2/3 with DBH in brainstem NA nuclei A7, LC, A5, sub CD/CV, anterior
153 C1/A1 and C2/A2, and posterior C1/A1 and C2/A2 (Figure 2A-C). No Vglut1/DBH double positive
154 neurons were detected in any part of the central NA system, consistent with our fate map. Vglut3
155 mRNA colocalization with DBH is only found in the posterior part of C2/A2 where 27.1 $\pm$ 1.86%
156 DBH^+ neurons have Vglut3 co-localization, again consistent with our fate map. For Vglut2, we
157 only found detectable levels of Vglut2 mRNA in C1/A1 and C2/A2 NA region, but not in A7, LC,
158 A5, sub CD/CV. Quantitatively, the percentage of Vglut2/DBH double positive neurons in anterior
159 C1/A1, anterior C2/A2, posterior C1/A1 and posterior C2/A2 is 84.7 $\pm$ 5.82%, 66.3 $\pm$ 0.335%, 35.7
160 $\pm$ 3.01% and 90.1 $\pm$ 2.45%, respectively. This result is consistent with the previous *in situ* data in
161 adult rats (DePuy et al., 2013; Stornetta et al., 2002a, 2002b) suggesting that there is no obvious
162 expression difference of Vglut2 in the central NA system between mouse and rat. However, the
163 Vglut2 *in situ* data did not show expression in anterior NA populations. This difference between
164 our *in situ* data and fate map data supports our previous hypothesis that many NA neurons
165 expressed Vglut2 at some point from early development toward adulthood but the expression of
166 Vglut2 is turned back down during adulthood. Interestingly, Yang et al. (2021) did show adult
167 Vglut2 co-expression in LC by a viral injection of both Cre and Flpo-dependent eYFP into the LC
168 of a bi-transgenic mouse with both TH-Flpo and Vglut2-Cre. To verify this result, we injected an
169 AAV virus containing Cre-dependent tdTomato (pAAV-EF1a-DIO-tdTomato-WPRE) into the LC
170 region of adult *Vglut2-Cre* mice. Consistent with Yang et al. (2021), we observed sparse Vglut2-
171 Cre and TH (immunopositive) double positive neurons in the LC (Figure 2 supplement 1).
172 Additionally, Souza et al. (2022a) showed about 28.5% A5 neurons are Vglut2 $mRNA^+$ in adult rats
173 by RNA scope, a method which is more sensitive than the traditional *in situ* hybridization we used

174 here. These data suggest that some adult NA neurons in LC and A5 have Vglut2 co-expression,
175 but the Vglut2 mRNA level cannot be detected by traditional *in situ* hybridization.
176
177 **Vglut2 expression is effectively knocked down in the whole central noradrenergic system in**
178 ***TgDBH-Cre/+; Vglut2$^{flox/flox}$* mice**
179 To investigate the requirement of Vglut2-based glutamatergic signaling in the central NA system
180 in breathing under physiological challenges, we used *TgDBH-Cre/+; Vglut2$^{flox/flox}$* as the mouse
181 model. This is the same model used by Abbott et al. (2014) to show that *Vglut2* expression in the
182 NA system was required for a modest increase in respiratory frequency following unilateral
183 optogenetic stimulation of anterior C1. To verify if Vglut2 expression is effectively removed from
184 central NA neurons in *TgDBH-Cre/+; Vglut2$^{flox/flox}$* mice, we carried out fluorescent RNA *in situ*
185 hybridization for Vglut2 and DBH in the mouse brainstems and compared the Vglut2 signal
186 intensity in DBH^{+} neurons in *TgDBH-Cre/+; Vglut2$^{flox/flox}$* and its littermate controls. We found that
187 Vglut2 mRNA expression is 96.4 $\pm$ 0.226% decreased compared to controls, indicating that the
188 Vglut2 is effectively recombined to abrogate expression in NA neurons (Figure 3A-B).
189
190 **Vglut2-based glutamatergic signaling in central NA neurons is not required for baseline**
191 **breathing nor for the hypercapnic ventilatory reflex under distinct CO_2 challenges**
192 Multiple prior studies provide indirect evidence that NA glutamate transmission may play roles
193 in respiratory function, particularly that anterior C1 neurons mediate the hypoxic ventilatory
194 response through the pFRG/RTN and/or the NA A5 group (Malheiros-Lima et al., 2022, 2020).
195 Additionally, the A5 group has been implicated in the hypercapnic reflex (Haxhiu et al., 1996).
196 Thus, we sought to determine if Vglut2-based glutamatergic signaling in central NA neurons is
197 necessary to regulate baseline breathing and the hypercapnic chemoreflex in awake and
198 unrestrained animals. We used whole-body barometric plethysmography to measure the
199 breathing and metabolism of conscious and free-moving mice. After a five-day habituation
200 protocol, the ventilation response of *TgDBH-Cre/+; Vglut2$^{flox/flox}$* mice and their littermate
201 controls was measured under room air and hypercapnia (5% CO_2) (Figure 4A). Surprisingly,
202 *TgDBH-Cre/+; Vglut2$^{flox/flox}$* mice didn't show significant differences in overall respiratory output

203 (V_E/V_{O2}), respiratory rate (V_f), tidal volume (V_T), minute ventilation (V_E) and metabolism demand
204 (V_{O2}) compared to their littermate controls under both room air and 5% CO_2 challenge (Figure 4B
205 and Table 1-2). These results suggested that Vglut2-based glutamatergic signaling is not required
206 for regulating baseline breathing and hypercapnic ventilatory reflex under 5% CO_2.
207
208 To further investigate if Vglut2-based glutamatergic signaling in central NA neurons is required
209 for ventilation response of higher CO_2 challenges, we also measured the breathing of *TgDBH-*
210 *Cre/+; Vglut2*$^{flox/flox}$ mice under 7% CO_2 and 10% CO_2. We found that under the 7% CO_2 condition,
211 *TgDBH-Cre/+; Vglut2*$^{flox/flox}$ mice showed only a significantly decreased tidal volume (V_T), but the
212 overall respiratory output (V_E/V_{O2}), respiratory rate (V_f), minute ventilation (V_E) and metabolism
213 demand (V_{O2}) didn't show a significant difference between the mutant mice and their sibling
214 controls (Figure 5A-B and Table 3). This result suggests that Vglut2-based glutamatergic signaling
215 in central NA neurons is not required or at least is not as important as previously expected for
216 regulating the hypercapnic ventilatory reflex under 7% CO_2.
217
218 Under 10% CO_2 challenge, none of the overall respiratory outputs (V_E/V_{O2}), respiratory rate (V_f),
219 tidal volume (V_T), minute ventilation (V_E) and metabolism demand (V_{O2}) were significantly
220 different between *TgDBH-Cre/+; Vglut2*$^{flox/flox}$ mice and their littermate controls, suggesting that
221 Vglut2-based glutamatergic signaling in central NA neurons is not required for the hypercapnic
222 ventilatory reflex under 10% CO_2 (Figure 6A-B and Table 4).
223
224 **Vglut2-based glutamatergic signaling in central NA neurons is not required for the hypoxic**
225 **ventilatory reflex under 10% O_2**
226 To determine if Vglut2-based glutamatergic signaling in central NA neurons is necessary to
227 regulate the hypoxic chemoreflex, we measured the ventilation response of *TgDBH-Cre/+;*
228 *Vglut2*$^{flox/flox}$ mice under 10% O_2. We analyzed the five respiratory parameters in three 5-min time
229 periods under 10% O_2 challenge. No significant difference was found in the overall respiratory
230 output (V_E/V_{O2}), respiratory rate (V_f), tidal volume (V_T), minute ventilation (V_E) and metabolism
231 demand (V_{O2}) between *TgDBH-Cre/+; Vglut2*$^{flox/flox}$ mice and controls in either of the three 5-min

232 10% O_2 periods (Figure 7A-B and Table 5). These data suggest that Vglut2-based glutamatergic
233 signaling in central NA neurons is not required for the hypoxic ventilatory reflex under 10% O_2.
234
235 **Discussion**
236 Neuron co-transmission of two or more neurotransmitters across excitatory, inhibitory, and
237 neuro-modulatory facets is becoming an increasingly appreciated phenomenon in the central
238 nervous system. Functional interrogation of co-transmission is essential not only to understand
239 the distinct and cooperative roles that multiple signaling molecules may play at the synapse but
240 also to determine the most critical targets for potential therapeutics. To our knowledge, the
241 unopposed paradigm in the field until now has been that vesicular glutamate transporter 2
242 (Vglut2)-based glutamate transmission from central noradrenergic neurons is important in
243 respiratory homeostasis. Anatomically, it has long been appreciated that central NA neurons co-
244 express Vglut2, the major glutamate marker among three glutamate transporters (DePuy et al.,
245 2013; Souza et al., 2022a; Stornetta et al., 2002a, 2002b; Yang et al., 2021). Also, it has been well
246 documented that NA Vglut2 positive fibers innervate known central respiratory centers or other
247 autonomic centers, that, when perturbed, could disrupt respiratory homeostasis (Supplemental
248 Table 1). Functionally, multiple reports have argued that Vglut2-based glutamate transmission
249 plays a role in respiratory homeostasis. It has also been suggested that, at least for C1 neurons,
250 the apparent lack of a plasmalemmal monoamine transporter may attenuate or eliminate
251 noradrenergic or adrenergic release from these fibers. However as discussed below, much of the
252 functional evidence supporting a role for Vglut2-based glutamate transmission from central
253 noradrenergic neurons is circumstantial or of a non-physiological nature, and absent or
254 attenuated release of adrenaline and noradrenaline has not been demonstrated. Nonetheless,
255 the dominant perspective that NA-Vglut2 glutamate transmission plays a role in breathing has
256 remained unchallenged. Our studies here uncover a novel dynamic expression pattern for Vglut2
257 and an entirely undescribed co-expression domain for Vglut3 in the central NA neurons, and in
258 contrast to prior work, our results show that loss of Vglut2 in NA neurons does not appreciably
259 change baseline or chemosensory breathing in conscious and free-moving mice.
260

261 Vglut2 has been shown to be co-expressed in subsets of central NA neurons, however, to our
262 knowledge, the potential for the central NA neurons to express the other glutamate transporters
263 Vglut1 or Vglut3 has not been reported at the anatomical level. To determine if central NA
264 neurons express either Vglut1 or Vglut3 and to confirm the Vglut2 expression, we carried out
265 cumulative intersectional fate mapping using *Vglut1-Cre/+; DBH-p2a-Flpo/+; RC::FLTG/+, Vglut2-*
266 *Cre/+; DBH-p2a-Flpo/+; RC::FLTG/+ and Vglut3-Cre/+; DBH-p2a-Flpo/+; RC::FLTG/+* compound
267 mouse lines. As this approach maps the cumulative history of expression, we also examined acute
268 adult expression of Vglut1, Vglut2 and Vglut3 using fluorescent RNA *in situ* hybridization. Our *in*
269 *situ* results for Vglut2 agreed with earlier published outcomes (DePuy et al., 2013; Stornetta et
270 al., 2002a, 2002b) showing as much as 80% expression in posterior NA neurons. However, there
271 was no appreciable signal in anterior groups (A7, LC, A5, sub CD/CV). This lack of expression was
272 in stark contrast to the cumulative fate map for Vglut2, showing as much as 75% of the anterior
273 central NA neurons were recombined by the *Vglut2-Cre* over the lifetime of the animal. To further
274 interrogate the acute activity of the *Vglut2-Cre* in the Locus Coeruleus in the adult mouse, we
275 injected a Cre responsive virus in LC of *Vglut2-Cre* mice. The outcomes from the cumulative fate
276 map and acute injections are in agreement with published results from Yang et al. (2021).
277 Notably our use of the *DBH-p2a-Flpo* avoided expression in the PBN that was seen in the *TH-Flp*
278 mouse. In addition, 28.5% A5 neurons were shown to be Vglut2^{+} in adult rats by RNA scope (Souza
279 et al., 2022b). It is notable that both our lab and work published by (DePuy et al., 2013; Stornetta
280 et al., 2002a, 2002b) failed to detect Vglut2 expression in anterior groups, but that apparently
281 very low levels can be detected by more sensitive recombinase and RNA scope methods.
282 Additional electrophysiological evidence suggests that this expression is functional (Yang et al.,
283 2021). Our data suggests that Vglut2 co-expression in anterior NA groups is time dependent,
284 though the underlying temporal dynamics of Vglut2 remain unknown. It is notable that we see
285 nearly 80% of the LC and 85% of A5 recombined in the intersectional strategy representing
286 lifetime expression, but our and other studies find only 20% of the LC and 28.5% of A5 may be
287 expressing Vglut2 at any given moment in adults. This suggests either a temporal restriction in
288 expression as the animal matures or may reflect dynamic change driven by behavioral or
289 physiological experiences.

290 For Vglut1, neither fate map nor *in situ* hybridization revealed any co-expression within the
291 central NA system. However, Vglut3 expression was found in the posterior part of NA neurons
292 including C2/A2 and C1/A1, which is first characterized by this study. The majority of this Vglut3
293 co-expression is restricted to the posterior part of the C2/A2 NA population. This NA region has
294 not been heavily implicated in respiratory control nonetheless it readily lends itself to
295 interrogation by intersectional genetic methods and *in situ* hybridization. Given its distal
296 expression from anterior C1, it is unlikely that Vglut3 would compensate for loss of Vglut2 in
297 anterior C1, though this has not been ruled out. Further, while Vglut3 is a marker of glutamatergic
298 neurons, its role in neurotransmission is not wholly defined as Vglut3 is typically found in soma
299 and dendrites (Fremeau et al., 2004).
300
301 Based on the Vglut2 co-expression in NA neurons and their projections to multiple brain regions
302 important in respiration, several studies suggest that glutamate in NA populations is important
303 in breathing control. Those studies provide a mix of circumstantial, indirect, or limited evidence
304 for the potential role of Vglut2-based glutamatergic signaling in central NA neurons in breathing
305 regulation. However, it has not yet been shown whether or not NA-based Vglut2 signaling is
306 required for respiratory control due to experimental caveats or limitations.
307
308 Abbott et al. (2014) showed that conditionally knocking out Vglut2 in the whole central NA
309 system attenuated a modest increase in respiratory rate resulting from unilateral C1 optogenetic
310 stimulation. Absolute values and other respiratory parameters, including tidal volume (V_T) and
311 minute ventilation (V_E) were not reported, making direct comparison difficult. While the
312 optogenetic stimulation did drive a Vglut2 dependent increase in respiratory rate, it is not clear
313 if the resulting change in breathing reflects a native feature of the network that might be engaged
314 in chemosensory responses, exercise, or volitional control. Thus, it remains possible that strong
315 optogenetic stimulation of a small, isolated population drives a Vglut2 dependent but ectopic
316 function that is not typically engaged in the normal operation of the breathing network. Such
317 ectopic outcomes could come from several potential, non-exclusive mechanisms. First, unilateral
318 stimulation could drive a network hysteresis or dysregulation akin to a focal injury that is not a

319 typical biological feature (Ducros et al., 2003). This point is well made in Abbott et al. (2013) in
320 their discussion of C1 optogenetic stimulation where they state, “resulting cardiorespiratory
321 response pattern should not be considered strictly “physiological,” because a physiological
322 response is never initiated by selective activation of a single cluster of CNS neurons and the
323 various subsets of C1 neurons are presumably never recruited en bloc under any physiological
324 condition”. Second, strong stimulation could result in overwhelming synaptic mechanisms (i.e.,
325 glial uptake) resulting in glutamate spillover and unintended cross talk to affect extra-synaptic
326 neurons proximal to targeted NA fibers. Activity dependent spillover transmission has been
327 documented elsewhere in the nervous system (Henneberger et al., 2020; Hülsmann et al., 2000).
328 Third, the outcomes could be secondary to a different autonomic or behavioral function requiring
329 NA-derived glutamatergic signaling involving metabolism or circulation (DePuy et al., 2013; Yang
330 et al., 2021).
331
332 More circumstantially, Malheiros-Lima et al. (2020) suggested C1 neurons potentially release
333 glutamate at the pFRG site to regulate breathing under hypoxia by providing three indirect lines
334 of evidence: 1) Vglut2-expressing C1 neurons project to the pFRG region; 2) Increased breathing
335 was blunted after blockade of ionotropic glutamatergic receptors at the pFRG site under
336 anesthesia using chemical hypoxia; 3) Depletion of C1 neurons eliminated the increased
337 breathing elicited by hypoxia. However, 1) the glutamatergic signaling targeting the pFRG region
338 is not necessarily from C1 NA neurons since glutamatergic neurons from other regions also
339 project to the pFRG site (Yang and Feldman, 2018).Thus, it is possible that the glutamatergic
340 signaling that is required for hypoxic response is derived from other glutamatergic neurons such
341 as the preBötzinger complex and the RTN itself; 2) C1 neuron depletion knocks out all the
342 signaling modalities in the C1 population including both noradrenaline and glutamate. It is not
343 clear which signaling drives the hypoxic response.
344
345 Similarly, Malheiros-Lima et al. (2022) and Malheiros-Lima et al. (2018) showed that Vglut2-
346 expressing C1 neurons project to the NA A5 region and the preBötzinger complex respectively.
347 The blockade of ionotropic glutamatergic receptors at the A5 region or preBötzinger complex

348 reduced the increase in phrenic nerve activities or the breathing frequency caused by
349 optogenetic stimulation of C1 cells in anesthetized preparation. Together these results suggest
350 that Vglut2-expressing C1 neurons communicate with A5 or preBötzinger complex neurons by
351 releasing glutamate in turn to regulate phrenic nerve activities or breathing frequency. Again,
352 these two studies showed that C1 neurons are important to regulate phrenic nerve activities or
353 breathing frequency, however, it is not necessarily through a direct C1-A5 or C1-preBötzinger
354 complex glutamatergic pathway, whereas an indirect multi-synaptic pathway originating with C1
355 noradrenaline and ending with glutamate transmission from an intermediate to A5 or
356 preBötzinger complex cannot be ruled out. Importantly, in all four studies noted here, respiratory
357 measurements were limited or proxies of breathing under anesthesia were used. The role of NA-
358 Vglut2 signaling was not reported in the context of an awake, unrestrained animal under
359 normoxic, hypoxic, or hypercapnic breathing.
360
361 Thus, the limitations and indirect lines of the evidence in these studies raised the question as to
362 whether or not glutamatergic signaling in central NA neurons is required or necessary to
363 modulate respiratory homeostasis under more physiologically relevant circumstances and if NA-
364 derived glutamate is an important mechanism to understand the pathophysiology of NA neurons
365 in respiratory diseases. The goal of our study was to test the requirement of NA-based
366 glutamatergic signaling in breathing homeostasis in the awake and unrestrained animal under
367 conditions that would engage the whole respiratory control network rather than a singular
368 component that may drive hysteresis or artifactual outcomes. Our *in vivo* breathing data under
369 room air, hypoxic, and multiple hypercapnic conditions failed to show the requirement of NA-
370 derived Vglut2 in normal breathing and respiratory chemoreflexes directly. To ensure a rigorous
371 and robust conclusion, first we use exactly the same mouse model, *TgDBH-Cre/+; Vglut2*$^{flox/flox}$,
372 as Abbott et al. (2014) used, and confirmed, by a second method (fluorescent RNA *in situ*
373 hybridization) that Vglut2 expression was indeed abrogated in the whole central NA system. Our
374 results are in strong agreement with DePuy et al. (2013) that recombination is efficient. Notably,
375 we assayed for expression at the cell body, rather than the fibers and see no singular cell body
376 that is scored positive. Second, we measured the breathing of conscious, unrestrained, and

377 habituated mice under physiological challenges including normoxia, hypercapnia and hypoxia.
378 Third, multiple respiratory and metabolic parameters were measured and reported in absolute
379 values including respiratory rate, tidal volume, minute ventilation, oxygen consumption, overall
380 respiratory output (minute ventilation normalized to oxygen consumption) in order to visualize
381 breathing function comprehensively. Fourth, our experimental design was overpowered (i.e.,
382 n=16-21 vs 5-13 needed for power based on power analysis and n=7-8 reported in other
383 manuscripts). Each respiratory/metabolic parameter for each physiological condition including
384 room air, hypercapnia, and hypoxia was derived by quantifying the entire respiratory trace and
385 analyzed between mutant and sibling controls by using a powerful linear mixed-effects
386 regression model with animal type (experimental vs. control) as fixed effects, animal ID as a
387 random effect and including sex as a variable (there was no sex specific effect) (Lusk et al., 2022).
388
389 Despite our experimental design and the extensive nature of our measurements, there remain
390 several considerations in the interpretation of our data. First, we uncovered a novel NA co-
391 expressed glutamate transporter, Vglut3. It remains a formal possibility that Vglut3 somehow
392 compensates for the loss of Vglut2, however we argue that this is unlikely for the following
393 reasons. First, our model is the same used in the other study where an effect was seen with
394 optogenetic stimulation. Second, focus has been on anterior C1 whereas Vglut3 is expressed in
395 the posterior CA domains. Another consideration is that pre- or post-natal developmental
396 compensation corrects for the loss of NA derived glutamate. Again, we argue that is not likely, as
397 we are using the same adult model that provided the most direct evidence and first functionally
398 demonstrated a potential role for C1-derived glutamate in breathing. Second, Abbott et al.
399 (2014) highlight that Vglut2 negative NA neurons showed no obvious abnormalities in number,
400 morphology, and projection patterns. Third, we have examined the requirement of NA-expressed
401 Vglut2 in P7 neonate mice in the auto-resuscitation reflex and saw no differences (data not
402 shown). However, this could be better tested by using the *TgDBH-CreER* (Stubbusch et al., 2011)
403 to more acutely remove Vglut2 expression (though this leaves a window of 2-3 weeks for
404 compensation to occur). Yet another consideration in interpreting our results is that we only
405 address the loss of NA-Vglut2 based signaling across the entire NA system. It remains a formal

406 possibility that we have removed Vglut2 dependent signaling from two counter balancing regions
407 of the NA system and are therefore left with null results whereas removal from anterior C1 alone
408 would show a requirement. To test this possibility, it would require an intersection conditional
409 approach, something that has not yet been shown to be efficient and effective and would be
410 beyond the scope of these studies. Additionally, in our studies, we account for potential
411 metabolic changes that may underlie or be coordinate with changes in breathing. However, in
412 this study we did not test for potential changes in blood pressure or other autonomic functions
413 as well as affective state that may, in some obscure way, compensate for changes in breathing.
414 Lastly, our results are loss of function in nature. We do not test sufficiency or gain of function and
415 cannot fully rule out a role for NA-Vglut2 based glutamatergic signaling in the control of
416 breathing.
417
418 From a translational perspective, our data questions whether or not glutamatergic signaling in
419 NA neurons is likely to be a key mechanism and therefore a therapeutic target for breathing
420 disorders, such as Rett syndrome and SIDS. *Mecp2*-deficient mice (a mouse model of Rett
421 Syndrome that phenocopies many human symptoms) showed both a deficiency of NA
422 populations (reduced number of NA neurons in C2/A2 and C1/A1 group) and highly variable
423 respiratory rhythm at around 4-5 weeks of age (Roux et al., 2007; Viemari et al., 2005). 80% Rett
424 Syndrome patients experience breathing issues, such as unstable breathing, episodes of
425 hyperventilation and breathing holds, during the whole lifespan including both childhood and
426 adulthood (Ramirez et al., 2020). SIDS decedents show NA abnormalities and are hypothesized
427 to ultimately succumb from a failure in cardiorespiratory autoresuscitation (Chigr et al., 1989;
428 Garcia et al., 2013; Kopp et al., 1993; Mansouri et al., 2001; Ozawa et al., 2003; Takashima and
429 Becker, 1991). However, *TgDBH-Cre/+; Vglut2*$^{flox/flox}$ mice, have normal baseline and
430 chemosensory respiratory parameters as adults and neonate mice show normal
431 autoresuscitation indicating that perturbed NA based glutamatergic signaling may not be a key
432 driver in these or other related respiratory pathophysiologies.
433

434 In conclusion, our studies demonstrated the extent of glutamate as a functional vesicular
435 glutamate transporter co-expression in central noradrenergic system. We were able to
436 characterize a novel Vglut3-expressing NA population in the posterior C2/A2 nuclei and found a
437 different Vglut2 co-expression pattern in anterior NA groups from a cumulative intersectional
438 fate map compared to a viral fate map and *in situ* hybridization in the adult, suggesting that
439 anterior NA populations may have a time-dependent or experience-dependent manner for
440 Vglut2 expression. Furthermore, despite prior studies providing indirect and circumstantial
441 evidence that noradrenergic-based glutamatergic signaling may play a role in control of
442 breathing, our studies that remove Vglut2 expression from noradrenergic neurons failed to
443 perturb room air breathing, the hypercapnic ventilatory reflex, and the hypoxic ventilatory reflex,
444 which challenges the current dominant perspective and provides further insight into the
445 potential role of NA-glutamate transmission in the control of breathing. Based on our data, we
446 suggest that noradrenergic-based glutamatergic signaling is not required for regulating baseline
447 breathing or the hypercapnic and hypoxic respiratory chemoreflexes, and glutamate may not be
448 a critical mechanistic component of NA neuron dysfunction in respiratory disorders.
449

450 **Materials and Methods**

451 **Ethical Approval**

452 Studies were approved by the Baylor College of Medicine Institutional Animal Care and Use
453 Committee (IACUC) under protocol AN-6171, and all experiments reported here were performed
454 in accordance with relevant guidelines and regulations.
455

456 **Breeding, Genetic Background, and Maintenance of Mice**

457 We maintained all our heterozygous mouse strains by backcrossing to wildtype C57BL/6J mice
458 and homozygous mouse strains by sibling crosses. For immunofluorescence experiments,
459 heterozygous *Vglut1*-Cre *(Jax Stock No: 023527), Vglut2-Cre (Jax Stock No: 016963) and Vglut3-*
460 *Cre (Jax Stock No: 018147)* were mated with heterozygous *DBH-p2a-Flpo (MMRRC ID: 41575)*
461 (Sun and Ray, 2016) mice respectively to derive compound lines with both Cre and Flpo alleles
462 (*Vglut1-Cre/+; DBH-p2a-Flpo/+, Vglut2-Cre/+; DBH-p2a-Flpo/+, and Vglut3-Cre/+; DBH-p2a-*

463 *Flpo/+*). Then these three compound lines were each mated with homozygous
464 *RC::F_TdTomato_P_GFP (RC::FLTG, Jax Stock No: 026932)* to derive three different intersectional
465 mouse lines *Vglut1/Cre/+; DBH-p2a-Flpo/+; RC::FLTG/+, Vglut2/Cre/+; DBH-p2a-Flpo/+;*
466 *RC::FLTG/+ and Vglut3/Cre/+; DBH-p2a-Flpo/+; RC::FLTG/+.* For *in situ* hybridization experiments,
467 wildtype C57BL/6J mice were ordered from the Center of Comparative Medicine (CCM), Baylor
468 College of Medicine. For NA-Vglut2 conditional loss of function *in situ* hybridization and
469 plethysmography experiments, hemizygous *TgDBH-Cre (MMRRC ID: 036778-UCD GENSAT)* mice
470 were mated with homozygous *Vglut2$^{flox/flox}$ (Jax Stock No: 012898)* to derive *TgDBH-Cre;*
471 *Vglut2$^{flox/+}$*. *TgDBH-Cre; Vglut2$^{flox/+}$* mice were mated with *Vglut2$^{flox/flox}$* to derive *TgDBH-Cre;*
472 *Vglut2$^{flox/flox}$*. Sibling mice that lacked the Cre allele or carried the Cre allele but lacked the floxed
473 Vglut2 alleles were used as controls. Rosa26 specific primers for the *RC::FLTG* mice were 5'-
474 GCACTTGCTCTCCCAAAGTC, 5'-GGGCGTACTTGGCATATGAT, and 5'-CTTTAAGCCTGCCCAGAAGA
475 (Ray et al., 2011) and yield a 495 bp band (targeted) and 330 bp band (wt). Cre-specific primers
476 for all Cre drivers were 5'-ATCGCCATCTTCCAGCAGGCGCACCATTGCCC and 5'-
477 GCATTTCTGGGGATTGCTTA and yielded a 550 bp band if positive. Flpo-specific primers for *DBH-*
478 *p2a-Flpo* are 5'- CACGCCCAGGTACTTGTTCT and 5'-CCACAGCAAGAAGATGCTGA (Sun and Ray,
479 2016) and yielded a 226 bp band if positive. Vglut2^{flox} specific primers for Vglut2-floxed mice are
480 available at The Jackson Laboratory website (https://www.jax.org/strain/012898).
481
482 **Immunofluorescence staining**
483 *Vglut1, Vglut2, or Vglut3-Cre/+; DBH-p2a-Flpo/+; RC::FLTG/+* adult mice were sacrificed and
484 transcardially perfused with 0.1 M phosphate-buffered saline (PBS) then with 4%
485 paraformaldehyde (PFA) in PBS. Mouse brains were dissected out and fixed for 2h in 4% PFA
486 before a PBS rinse and dehydration in 30% sucrose in PBS. Brains were embedded in OCT blocks,
487 sectioned at the thickness of 30µm, mounted on slides, and stored at -80°C until they were ready
488 for staining. The slides were hydrated in 0.1% Triton-X in PBS (PBST) for 15 mins, blocked with 5%
489 donkey serum in 0.1% PBST for 1h at room temperature and then incubated with primary
490 antibodies for 72 hours at 4°C in 0.1% PBST with 5% donkey serum. Tissues were washed in 0.1%
491 PBST 3 times for 10 min each and then incubated with secondary antibodies for 2hs at room

492 temperature in 0.1% PBST with 5% donkey serum. Slides were washed with 0.1% PBST for 10 min
493 and washed in PBS twice for 10 min each, stained for DAPI, washed 3 times for 10 min each with
494 PBS and mounted in ProLong Glass (Invitrogen). The following primary and secondary antibodies
495 were used: chicken anti-GFP (1:1,000, Abcam ab13970), rabbit anti-dsRed (1:1,000, Clontech
496 632496), donkey anti-chicken Cy2 (1:500, Jackson 703-225-155), donkey anti-rabbit Cy3 (1:500,
497 Jackson 711-165-152).
498
499 **In situ hybridization**
500 Mouse brains were dissected out from adult mice with 6-8 week of age, sectioned into
501 25µm brain sections and mounted on slides. We generated a digoxigenin (DIG)-labeled
502 mRNA antisense probe against *Vglut1, Vglut2, and Vglut3* and fluorescein (FITC)-labeled mRNA
503 against *DBH* using reverse-transcribed mouse cDNA as a template and an RNA DIG or FITC-
504 labeling kits from Roche (Sigma). Primer and probe sequences for the *Vglut1, Vglut2, Vglut3* and
505 *DBH* probes are available in the Allen Brain Atlas (http://www.brain-map.org). For the Vglut2 and
506 DBH double ISH in *TgDBH-Cre/+; Vglut2*$^{flox/flox}$ and their littermate controls, we generated a new
507 Vglut2 probe targeting exon 2 of Vglut2 specifically (Tong et al., 2007) and the probe sequence is
508 892-1144bp as Slc17a6 transcript variant 1 and the size is 253bp. ISH was performed by the
509 RNA In Situ Hybridization Core at Baylor College of Medicine using an automated robotic
510 platform as previously described (Yaylaoglu et al., 2005) with modifications of the protocol for
511 double ISH. Modifications in brief (see Yaylaoglu et al. (2005) for buffer descriptions): both
512 probes were hybridized to the tissue simultaneously. After the described washes and blocking
513 steps the DIG-labeled probes were visualized using tyramide-Cy3 Plus (1/75 dilution, 15-minute
514 incubation, Akoya Biosciences). After washes in TNT, the remaining HRP-activity was quenched
515 by a 10-minute incubation in 0.2M HCl. The sections were then washed in TNT, blocked in TNB
516 for 15 minutes, and incubated at room temperature for 30 minutes with HRP-labeled sheep anti-
517 FITC antibody (1/500 in TNB, Roche/Sigma). Following washes in TNT, the FITC-labeled probe was
518 visualized using tyramide-FITC Plus (1/50 dilution, 15-minute incubation, Akoya Biosciences).
519 Following washes in TNT, the slides were stained with DAPI (invitrogen), washed again, removed
520 from the machine, and mounted in ProLong Diamond (Invitrogen).

521 **Viral Injection**

522 To verify Vglut2 co-expression in LC in adult mice (Yang et al., 2021), 6-week-old *Vglut2-Cre* mice
523 were injected with pAAV-EF1a-DIO-tdTomato-WPRE virus (RRID:Addgene_133786, obtained
524 from Joshua Ortiz at the Optogenetics and Viral Vectors Core at the Jan and Dan Duncan
525 Neurological Research Institute, 1ul at 7.90E+10 Gc/mL) into the LC (coordinates from bregma
526 anteroposterior −5.4 mm, lateral + 0.8 mm and dorsoventral – 4.0 mm) and allowed to incubate
527 for 4 weeks.

528

529 **Plethysmography**

530 Plethysmography on conscious and free-moving mice was carried out as described in (Ray et al.,
531 2011) on 6-8-week-old adult animals with at least 16 animals in both the experimental and
532 control group for each experiment. Animals were subjected to a five-day habituation protocol
533 with each day including several minutes of handling, temperature taken by rectal probe and at
534 least 30 min exposure in the plethysmography chamber (Martinez et al., 2019). Plethysmography
535 was then performed for each mouse within 1 week of the last day of habituation. On the day of
536 testing, mice were taken out from their home cage, weighed, and rectal temperature was taken.
537 Animals were then placed into a flow-through, temperature-controlled (about 32°C with real-
538 time temperature recording) plethysmography chamber and allowed to acclimate for at least 45
539 min in room air (21% O_2/79% N_2) conditions. After acclimation and measurement under room
540 air, the chamber gas was switched to a hypercapnic or hypoxic mixture of 5% CO_2/21% O_2/74%
541 N_2, 7% CO_2/21% O_2/72% N_2, 10% CO_2/21% O_2/69% N_2, or 10% O_2/90% N_2, depending on the
542 protocol, for 20 min. Chamber gas was then switched back to room air for another 20 min. The
543 animals were removed from the chamber and rectal temperature was measured immediately
544 after the mice were taken out from the chamber.

545

546 **Plethysmography data analysis and statistics**

547 Details were previously described in (Martinez et al., 2019; Ray et al., 2011). Plethysmography
548 pressure changes were measured using a Validyne DP45 differential pressure transducer, CD15
549 carrier demodulator and a reference chamber, and were recorded with LabChart Pro in real time.

550 Respiratory waveforms were analyzed by the BASSPRO module of the Breathe Easy software to
551 determine respiratory frequency (V_f), tidal volume (V_T), minute ventilation (V_E), oxygen
552 consumption (V_{O2}) and ventilatory equivalents for oxygen (V_E/V_{O2}) (Lusk et al., 2022). A power
553 analysis was performed using the reported effect size in Abbott et al. (2014) which used the same
554 mouse model as we used here and 5-13 mice were necessary to observe a statistically significant
555 result (Abbott et al. (2014) was able to see a significant difference between two groups with n=7
556 mice). In our experiments, the sample size for each group (*TgDBH-Cre/+; Vglut2*$^{flox/flox}$ and
557 control) exceeded 13. Results (V_f, V_E, V_T, V_{O2}, V_E/V_{O2}) for room air and hypercapnic or hypoxic
558 data were compared between *TgDBH-Cre/+; Vglut2*$^{flox/flox}$ cohorts and sibling controls using a
559 linear mixed-effects regression model with animal type (experimental vs. control) as fixed effects
560 and animal ID as a random effect (Lusk et al., 2022). A $p < 0.05$ was used to indicate statistical
561 significance, and individual data points, mean, and standard error of the mean are shown on all
562 charts. The graphs were plotted by Prism 8.
563
564 **Image quantification**
565 Images were taken by using a Zeiss upright epifluorescent microscope and a Zeiss LSM 880 with
566 Airyscan FAST confocal microscope. Images were captured using Zen software with z-stack
567 function from top to bottom with 0.34µm intervals, exported, and then analyzed in Imaris using
568 the spots and surface functions. For quantification of immunofluorescence staining, each GFP$^+$
569 area coincident with DAPI (to denote nuclear localization) was defined as Vglut2 or Vglut3-
570 expressing NA neurons while each tdTomato$^+$ area coincident with DAPI was defined as NA
571 neurons without any Vglut2 or Vglut3 co-expression. For quantification of Vglut2 or Vglut3 with
572 DBH double *in situ* hybridization in adult WT mice, DBH$^+$ areas coinciding with DAPI were
573 identified as NA neurons and the DBH$^+$ areas overlapped with Vglut2/3$^+$ pixels and DAPI were
574 defined as NA neurons colocalized with Vglut2/3. The number of Vglut2/3$^+$ NA neurons and
575 Vglut2/3$^-$ NA neurons was counted in each image for both immunofluorescence and in situ
576 experiments and the percentage of Vglut2/3$^+$ NA neurons among all NA neurons in each NA
577 nucleus in each mouse brainstem was calculated every other brain section unilaterally. For
578 quantification of Vglut2 and DBH double ISH in *TgDBH-Cre/+; Vglut2*$^{flox/flox}$ and their littermate

579 controls, Vglut2 pixel intensities in DBH$^+$ areas coincident with DAPI (NA neurons) were measured
580 in mutant and control images separately. The Vglut2 pixel intensity in NA neurons of control
581 brains was normalized as 1 and the relative Vglut2 pixel intensity of NA neurons in mutant brains
582 compared to that in control brains was calculated. At least three mouse brains were examined
583 for each set of experiments in each group. All quantitative results were graphed using Prism 8.
584
585 **Data availability**
586 All the data supporting this study is available from the corresponding author upon request.
587
588 **Acknowledgments**
589 We thank the Optical Imaging & Vital Microscopy Core (OiVM) at Baylor College of Medicine with
590 the expert assistance of Jason Kirk for confocal imaging. We thank BCM Neuropathology Core
591 and Tao Lin for tissue sectioning. We thank the RNA In Situ Hybridization Core at Baylor College
592 of Medicine with the expert assistance of Cecilia Ljungberg for performing in situ hybridization
593 (NIH S10 OD016167 and NIH IDDRC Grant P50 HD103555). We thank Dr. Joshua Ortiz and Dr.
594 Benjamin Arenkiel at the NRI Optogenetics and Viral Vectors Core for providing Cre-responsive
595 AAV virus used in viral injection.
596
597 **Author contributions**
598 YC designed and completed immunofluorescence staining, imaging, and plethysmography
599 experiments, analyzed data, and prepared the manuscript.
600 SL completed the viral injection experiments.
601 RR conceptualized and designed the study, analyzed the data, and prepared the manuscript.
602
603 **Competing interests**
604 No competing interests are declared.
605
606 **Figure 1. Cumulative fate maps of glutamate co-expressing NA neurons characterized by**
607 **intersectional genetics.** (A) Breeding schematic. *Vglut1-Cre/+*, *Vglut2-Cre/+* and *Vglut3-Cre/+*

608 were each bred with *DBH-p2a-Flpo/+* mice respectively. These *Vglut1, Vglut2, or Vglut3-Cre/+;*
609 *DBH-p2a-Flpo/+* compound lines were then crossed with the *RC::F_TdTomato_P_GFP*
610 intersectional reporter mice (*RC::FLTG*). In each of the three intersectional reporter crosses, NA
611 neurons co-expressing either Vglut1, Vglut2, or Vglut3 are labeled by green fluorescent protein
612 (eGFP) while NA neurons without any Vglut1,2, or 3 expression are labelled by red fluorescent
613 protein (tdTomato). Shown as an example is the *Vglut2-Cre/+; DBH-p2a-Flpo/+ RC::FLTG*
614 intersectional reporter line. (B) Quantification of the percentage of Vglut2-coexpressing NA
615 neurons among NA neurons in each brainstem NA nuclei including A7, LC, A5, sub CD/CV, anterior
616 C1/A1 and C2/A2, posterior C1/A1 and C2/A2. (C) Quantification of the percentage of Vglut3-
617 coexpressing NA neurons among NA neurons in each NA nuclei. (D) Fluorescent expression of
618 tdTomato (red) and eGFP (green) in coronal sections of Vglut1, Vglut2, or Vglut3 intersectional
619 reporter lines in brainstem NA nuclei. Nucleus is labeled by DAPI (blue). Scale bar 50µm.
620
621 **Figure 2. Characterization of real time co-expression of Vglut1, Vglut2 and Vglut3 in brainstem**
622 **NA neurons in adult mice by fluorescent *in situ* hybridization.** (A) Representative images of
623 Vglut1, Vglut2, or Vglut3 and DBH double ISH in coronal sections of WT mice in all of brainstem
624 NA nuclei in adult mice. DBH (green), Vglut1/2/3 (red), DAPI (cyan). Scale bar 50µm. (B)
625 Quantification of the percentage of Vglut2 co-expression in NA neurons in each NA nuclei. (C)
626 Quantification of the percentage of Vglut3 co-expression in NA neurons in each NA nuclei.
627
628 **Figure 3. DBH with Vglut2 co-staining by fluorescent *in situ* hybridization confirms that Vglut2**
629 **expression is disrupted in the whole central NA system in *TgDBH-Cre/+; Vglut2$^{flox/flox}$* mice.** (A)
630 Representative images of Vglut2 and DBH double ISH in anterior C1/A1, posterior C1/A1, anterior
631 C2/A2 and posterior C2/A2 in control and *TgDBH-Cre/+; Vglut2$^{flox/flox}$* mice. DBH (green), Vglut2
632 (red), DAPI (cyan). Scale bar 20µm.(B) Quantification of intensity of Vglut2 signal in control and
633 *TgDBH-Cre/+; Vglut2$^{flox/flox}$* mice.
634
635 **Figure 4. Vglut2 conditional knockout in central noradrenergic neurons fails to alter baseline**
636 **breathing and the hypercapnic ventilatory reflex (5% CO_2).** (A) Mouse model schematic and

637 experimental protocol including habituation and hypercapnia protocol. (B) Under both room air
638 and hypercapnia (5% CO_2), *TgDBH-Cre/+; Vglut2$^{flox/flox}$* mice didn't show significant changes in
639 respiratory output (V_E/V_{O2}), minute ventilation (V_E), respiratory rate (V_f), tidal volume (V_T), and
640 metabolism demand (V_{O2}). Linear mixed-effects regression model, *p<0.05.
641
642 **Figure 5. Vglut2 conditional knockout in central noradrenergic neurons fails to alter the**
643 **majority of hypercapnic ventilation parameters and metabolism under 7% CO_2.** (A) Mouse
644 model schematic and experimental protocol including habituation and hypercapnia protocol. (B)
645 Knocking out Vglut2 in the whole NA system failed to alter ventilation (V_E/V_{O2}, V_f, V_E) and
646 metabolism (V_{O2}) but only showed a significantly reduce in V_T under 7% CO_2 condition. Linear
647 mixed-effects regression model, *p<0.05.
648
649 **Figure 6. Vglut2 conditional knockout in central noradrenergic neurons fails to alter the**
650 **hypercapnic ventilatory reflex (10% CO_2).** (A) Mouse model schematic and experimental
651 protocol including habituation and hypercapnia protocol. (B) Knocking out Vglut2 in the whole
652 NA system didn't significantly alter ventilation (V_E/V_{O2}, V_f, V_T, V_E) and metabolism (V_{O2}) under 10%
653 CO_2 condition. Linear mixed-effects regression model, *p<0.05.
654
655 **Figure 7. Vglut2 conditional knockout in central noradrenergic neurons fails to alter the hypoxic**
656 **ventilatory reflex (10% O_2).** (A) Mouse model schematic and experimental protocol including
657 habituation and hypoxia protocol. (B) Knocking out Vglut2 in the whole NA system didn't show
658 significant breathing changes including V_E/V_{O2}, V_E, V_f, V_T, and V_{O2} in either of the three five-minute
659 time periods under hypoxia (10% O_2). Linear mixed-effects regression model, *p<0.05.
660
661 **Figure 2 Supplement 1. Virus injection of Cre-dependent tdTomato into LC of *Vglut2-Cre* mice.**

662 **Table 1.** Respiratory and metabolic values under room air conditions and the statistical tests.

663 **Table 2.** Respiratory and metabolic values under 5% CO_2 conditions and the statistical tests.

664 **Table 3.** Respiratory and metabolic values under 7% CO_2 conditions and the statistical tests.

665 **Table 4.** Respiratory and metabolic values under 10% CO_2 conditions and the statistical tests.

666 **Table 5.** Respiratory and metabolic values under 10% O_2 conditions and the statistical tests.

667 **Supplemental table 1.** Vglut2$^+$ innervations from central noradrenergic neurons to the brain
668 nuclei important in breathing control.

669
670 **References**
671

672 Abbott SBG, DePuy SD, Nguyen T, Coates MB, Stornetta RL, Guyenet PG. 2013. Selective
673 optogenetic activation of rostral ventrolateral medullary catecholaminergic neurons
674 produces cardiorespiratory stimulation in conscious mice. *J Neurosci* **33**:3164–3177.
675 doi:10.1523/JNEUROSCI.1046-12.2013
676 Abbott SBG, Holloway BB, Viar KE, Guyenet PG. 2014. Vesicular glutamate transporter 2 is
677 required for the respiratory and parasympathetic activation produced by optogenetic
678 stimulation of catecholaminergic neurons in the rostral ventrolateral medulla of mice in vivo.
679 *Eur J Neurosci* **39**:98–106. doi:10.1111/ejn.12421
680 Beltrán-Castillo S, Olivares MJ, Contreras RA, Zúñiga G, Llona I, von Bernhardi R, Eugenín JL.
681 2017. D-serine released by astrocytes in brainstem regulates breathing response to CO2
682 levels. *Nat Commun* **8**:838. doi:10.1038/s41467-017-00960-3
683 Chigr F, Najimi M, Jordan D, Denoroy L, Pearson J, Tommasi M, Gilly R, Kopp N. 1989.
684 [Immunohistochemical absence of adrenergic neurons in the dorsal part of the solitary tract
685 nucleus in sudden infant death]. *C R Acad Sci III, Sci Vie* **309**:543–549.
686 Comer AM, Qi J, Christie DL, Gibbons HM, Lipski J. 1998. Noradrenaline transporter expression
687 in the pons and medulla oblongata of the rat: localisation to noradrenergic and some C1
688 adrenergic neurones. *Brain Res Mol Brain Res* **62**:65–76. doi:10.1016/s0169-328x(98)00241-1
689 Del Negro CA, Funk GD, Feldman JL. 2018. Breathing matters. *Nat Rev Neurosci* **19**:351–367.
690 doi:10.1038/s41583-018-0003-6
691 DePuy SD, Stornetta RL, Bochorishvili G, Deisseroth K, Witten I, Coates M, Guyenet PG. 2013.
692 Glutamatergic neurotransmission between the C1 neurons and the parasympathetic
693 preganglionic neurons of the dorsal motor nucleus of the vagus. *J Neurosci* **33**:1486–1497.
694 doi:10.1523/JNEUROSCI.4269-12.2013
695 Dick TE, Dutschmann M, Feldman JL, Fong AY, Hülsmann S, Morris KM, Ramirez JM, Smith JC,
696 Respiratory Neurobiology Consortium. 2018. Facts and challenges in respiratory
697 neurobiology. *Respir Physiol Neurobiol* **258**:104–107. doi:10.1016/j.resp.2015.01.014
698 Ducros L, Vahedi K, Similowski T, Bousser M-G, Payen D. 2003. Uncontrollable high-frequency
699 tachypnea in a case of unilateral medial medullary infarct. *Intensive Care Med* **29**:841–844.
700 doi:10.1007/s00134-003-1658-6
701 Feldman JL, Del Negro CA, Gray PA. 2013. Understanding the rhythm of breathing: so near, yet
702 so far. *Annu Rev Physiol* **75**:423–452. doi:10.1146/annurev-physiol-040510-130049

703 Fremeau RT, Voglmaier S, Seal RP, Edwards RH. 2004. VGLUTs define subsets of excitatory
704 neurons and suggest novel roles for glutamate. *Trends Neurosci* **27**:98–103.
705 doi:10.1016/j.tins.2003.11.005
706 Garcia AJ, Koschnitzky JE, Ramirez J-M. 2013. The physiological determinants of sudden infant
707 death syndrome. *Respir Physiol Neurobiol* **189**:288–300. doi:10.1016/j.resp.2013.05.032
708 Gauda EB, Cristofalo E, Nunez J. 2007. Peripheral arterial chemoreceptors and sudden infant
709 death syndrome. *Respir Physiol Neurobiol* **157**:162–170. doi:10.1016/j.resp.2007.02.016
710 Guyenet PG, Stornetta RL, Bochorishvili G, Depuy SD, Burke PGR, Abbott SBG. 2013. C1
711 neurons: the body's EMTs. *Am J Physiol Regul Integr Comp Physiol* **305**:R187-204.
712 doi:10.1152/ajpregu.00054.2013
713 Haxhiu MA, Yung K, Erokwu B, Cherniack NS. 1996. CO2-induced c-fos expression in the CNS
714 catecholaminergic neurons. *Respir Physiol* **105**:35–45. doi:10.1016/0034-5687(96)00034-5
715 Henneberger C, Bard L, Panatier A, Reynolds JP, Kopach O, Medvedev NI, Minge D, Herde MK,
716 Anders S, Kraev I, Heller JP, Rama S, Zheng K, Jensen TP, Sanchez-Romero I, Jackson CJ,
717 Janovjak H, Ottersen OP, Nagelhus EA, Oliet SHR, Stewart MG, Nägerl UV, Rusakov DA. 2020.
718 LTP induction boosts glutamate spillover by driving withdrawal of perisynaptic astroglia.
719 *Neuron* **108**:919-936.e11. doi:10.1016/j.neuron.2020.08.030
720 Hülsmann S, Oku Y, Zhang W, Richter DW. 2000. Metabotropic glutamate receptors and
721 blockade of glial Krebs cycle depress glycinergic synaptic currents of mouse hypoglossal
722 motoneurons. *Eur J Neurosci* **12**:239–246.
723 Kopp N, Chigr F, Denoroy L, Gilly R, Jordan D. 1993. Absence of adrenergic neurons in nucleus
724 tractus solitarius in sudden infant death syndrome. *Neuropediatrics* **24**:25–29. doi:10.1055/s-
725 2008-1071508
726 Lorang D, Amara SG, Simerly RB. 1994. Cell-type-specific expression of catecholamine
727 transporters in the rat brain. *J Neurosci* **14**:4903–4914. doi:10.1523/JNEUROSCI.14-08-
728 04903.1994
729 Lusk S, Ward CS, Chang A, Twitchell-Heyne A, Fattig S, Allen G, Jankowsky J, Ray R. 2022.
730 Breathe Easy, an automated respiratory data pipeline for waveform characteristic analysis.
731 *BioRxiv*. doi:10.1101/2022.12.02.518741
732 Malheiros-Lima MR, Silva JN, Souza FC, Takakura AC, Moreira TS. 2020. C1 neurons are part of
733 the circuitry that recruits active expiration in response to the activation of peripheral
734 chemoreceptors. *eLife* **9**. doi:10.7554/eLife.52572
735 Malheiros-Lima MR, Silva TM, Takakura AC, Moreira TS. 2022. A5 noradrenergic-projecting C1
736 neurons activate sympathetic and breathing outputs in anaesthetized rats. *Exp Physiol*
737 **107**:147–160. doi:10.1113/EP089691
738 Malheiros-Lima MR, Totola LT, Lana MVG, Strauss BE, Takakura AC, Moreira TS. 2018. Breathing
739 responses produced by optogenetic stimulation of adrenergic C1 neurons are dependent on
740 the connection with preBötzinger complex in rats. *Pflugers Arch* **470**:1659–1672.
741 doi:10.1007/s00424-018-2186-0
742 Mansouri J, Panigrahy A, Filiano JJ, Sleeper LA, St John WM, Kinney HC. 2001. Alpha2 receptor
743 binding in the medulla oblongata in the sudden infant death syndrome. *J Neuropathol Exp*
744 *Neurol* **60**:141–146.

745 Martinez VK, Saldana-Morales F, Sun JJ, Zhu PJ, Costa-Mattioli M, Ray RS. 2019. Off-Target
746 Effects of Clozapine-N-Oxide on the Chemosensory Reflex Are Masked by High Stress Levels.
747 *Front Physiol* **10**:521. doi:10.3389/fphys.2019.00521
748 Ozawa Y, Takashima S, Tada H. 2003. Alpha2-adrenergic receptor subtype alterations in the
749 brainstem in the sudden infant death syndrome. *Early Hum Dev* **75 Suppl**:S129-38.
750 doi:10.1016/j.earlhumdev.2003.08.016
751 Ramirez J-M, Karlen-Amarante M, Wang J-DJ, Bush NE, Carroll MS, Weese-Mayer DE, Huff A.
752 2020. The pathophysiology of rett syndrome with a focus on breathing dysfunctions.
753 *Physiology (Bethesda)* **35**:375–390. doi:10.1152/physiol.00008.2020
754 Ray RS, Corcoran AE, Brust RD, Kim JC, Richerson GB, Nattie E, Dymecki SM. 2011. Impaired
755 respiratory and body temperature control upon acute serotonergic neuron inhibition. *Science*
756 **333**:637–642. doi:10.1126/science.1205295
757 Roux J-C, Dura E, Moncla A, Mancini J, Villard L. 2007. Treatment with desipramine improves
758 breathing and survival in a mouse model for Rett syndrome. *Eur J Neurosci* **25**:1915–1922.
759 doi:10.1111/j.1460-9568.2007.05466.x
760 Souza GMPR, Stornetta DS, Vitali AJ, Wildner H, Zeilhofer HU, Campbell JN, Abbott SBG. 2022a.
761 Chemogenetic activation of noradrenergic A5 neurons increases blood pressure and visceral
762 sympathetic activity in adult rats. *Am J Physiol Regul Integr Comp Physiol* **323**:R512–R531.
763 doi:10.1152/ajpregu.00119.2022
764 Souza GMPR, Stornetta RL, Stornetta DS, Guyenet PG, Abbott SBG. 2022b. Adrenergic C1
765 neurons monitor arterial blood pressure and determine the sympathetic response to
766 hemorrhage. *Cell Rep* **38**:110480. doi:10.1016/j.celrep.2022.110480
767 Stornetta RL, Sevigny CP, Guyenet PG. 2002a. Vesicular glutamate transporter DNPI/VGLUT2
768 mRNA is present in C1 and several other groups of brainstem catecholaminergic neurons. *J*
769 *Comp Neurol* **444**:191–206. doi:10.1002/cne.10141
770 Stornetta RL, Sevigny CP, Schreihofer AM, Rosin DL, Guyenet PG. 2002b. Vesicular glutamate
771 transporter DNPI/VGLUT2 is expressed by both C1 adrenergic and nonaminergic
772 presympathetic vasomotor neurons of the rat medulla. *J Comp Neurol* **444**:207–220.
773 doi:10.1002/cne.10142
774 Stubbusch J, Majdazari A, Schmidt M, Schütz G, Deller T, Rohrer H. 2011. Generation of the
775 tamoxifen-inducible DBH-Cre transgenic mouse line DBH-CT. *Genesis* **49**:935–941.
776 doi:10.1002/dvg.20773
777 Sun JJ, Ray R. 2016. Generation of Two Noradrenergic-Specific Dopamine-Beta-Hydroxylase-
778 FLPo Knock-In Mice Using CRISPR/Cas9-Mediated Targeting in Embryonic Stem Cells. *PLoS*
779 *ONE* **11**:e0159474. doi:10.1371/journal.pone.0159474
780 Takashima S, Becker LE. 1991. Delayed dendritic development of catecholaminergic neurons in
781 the ventrolateral medulla of children who died of sudden infant death syndrome.
782 *Neuropediatrics* **22**:97–99. doi:10.1055/s-2008-1071424
783 Tong Q, Ye C, McCrimmon RJ, Dhillon H, Choi B, Kramer MD, Yu J, Yang Z, Christiansen LM, Lee
784 CE, Choi CS, Zigman JM, Shulman GI, Sherwin RS, Elmquist JK, Lowell BB. 2007. Synaptic
785 glutamate release by ventromedial hypothalamic neurons is part of the neurocircuitry that
786 prevents hypoglycemia. *Cell Metab* **5**:383–393. doi:10.1016/j.cmet.2007.04.001
787 Viemari J-C, Roux J-C, Tryba AK, Saywell V, Burnet H, Peña F, Zanella S, Bévengut M,
788 Barthelemy-Requin M, Herzing LBK, Moncla A, Mancini J, Ramirez J-M, Villard L, Hilaire G.

789 2005. Mecp2 deficiency disrupts norepinephrine and respiratory systems in mice. *J Neurosci*
790 **25**:11521–11530. doi:10.1523/JNEUROSCI.4373-05.2005
791 Viemari J-C. 2008. Noradrenergic modulation of the respiratory neural network. *Respir Physiol*
792 *Neurobiol* **164**:123–130. doi:10.1016/j.resp.2008.06.016
793 Yang B, Sanches-Padilla J, Kondapalli J, Morison SL, Delpire E, Awatramani R, Surmeier DJ. 2021.
794 Locus coeruleus anchors a trisynaptic circuit controlling fear-induced suppression of feeding.
795 *Neuron* **109**:823-838.e6. doi:10.1016/j.neuron.2020.12.023
796 Yang CF, Feldman JL. 2018. Efferent projections of excitatory and inhibitory preBötzinger
797 Complex neurons. *J Comp Neurol* **526**:1389–1402. doi:10.1002/cne.24415
798 Yaylaoglu MB, Titmus A, Visel A, Alvarez-Bolado G, Thaller C, Eichele G. 2005. Comprehensive
799 expression atlas of fibroblast growth factors and their receptors generated by a novel robotic
800 in situ hybridization platform. *Dev Dyn* **234**:371–386. doi:10.1002/dvdy.20441

Figure 1

A

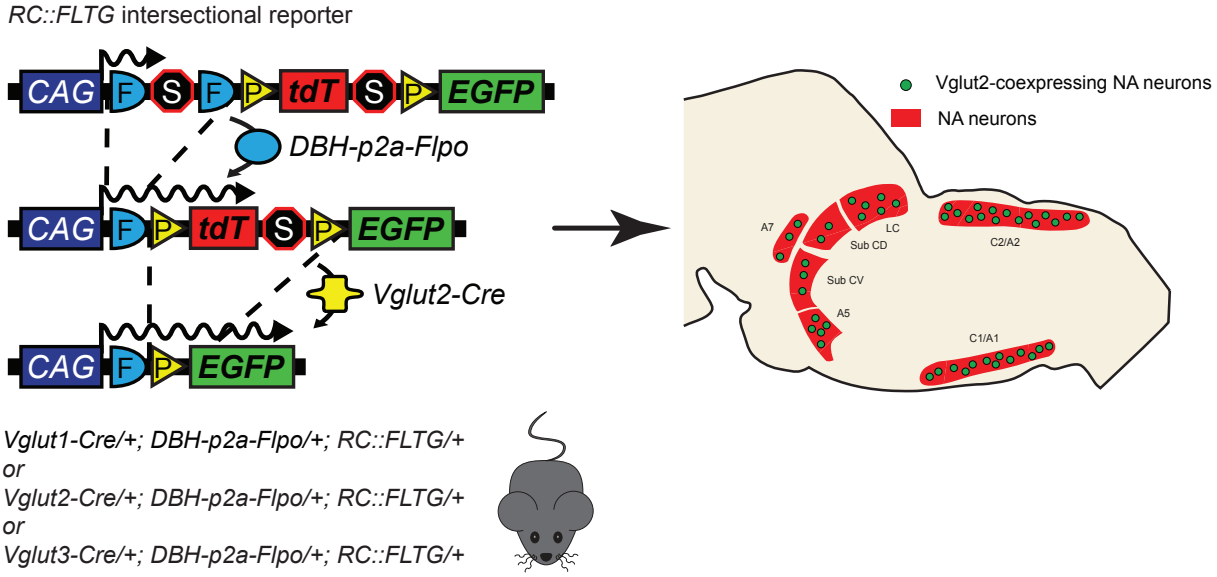
RC::FLTG intersectional reporter
CAG
F
S
F
P
tdT
S
P
EGFP
DBH-p2a-Flpo
CAG
F
P
tdT
S
P
EGFP
Vglut2-Cre
CAG
F
P
EGFP
Vglut2-coexpressing NA neurons
NA neurons
A7
LC
Sub CD
C2/A2
Sub CV
A5
C1/A1
Vglut1-Cre/+; DBH-p2a-Flpo/+; RC::FLTG/+
or
Vglut2-Cre/+; DBH-p2a-Flpo/+; RC::FLTG/+
or
Vglut3-Cre/+; DBH-p2a-Flpo/+; RC::FLTG/+

B

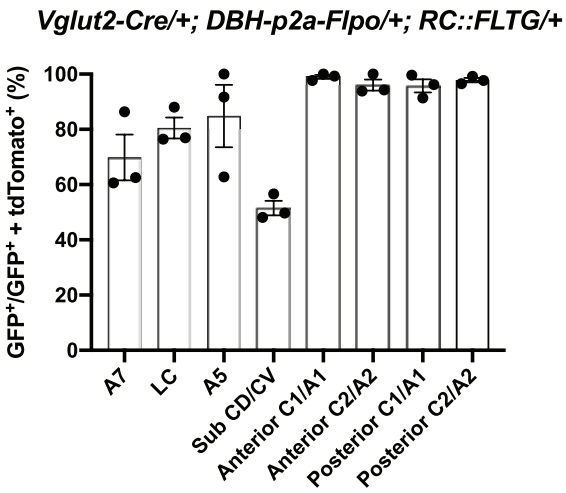
Vglut2-Cre/+; DBH-p2a-Flpo/+; RC::FLTG/+
GFP+/GFP+ + tdTomato+ (%)
100
80
60
40
20
0
A7
LC
A5
Sub CD/CV
Anterior C1/A1
Anterior C2/A2
Posterior C1/A1
Posterior C2/A2

C

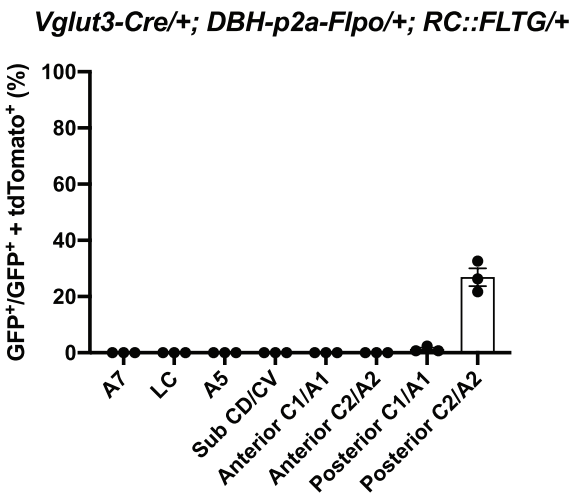
Vglut3-Cre/+; DBH-p2a-Flpo/+; RC::FLTG/+
GFP+/GFP+ + tdTomato+ (%)
100
80
60
40
20
0
A7
LC
A5
Sub CD/CV
Anterior C1/A1
Anterior C2/A2
Posterior C1/A1
Posterior C2/A2

Figure 1. cont.

D

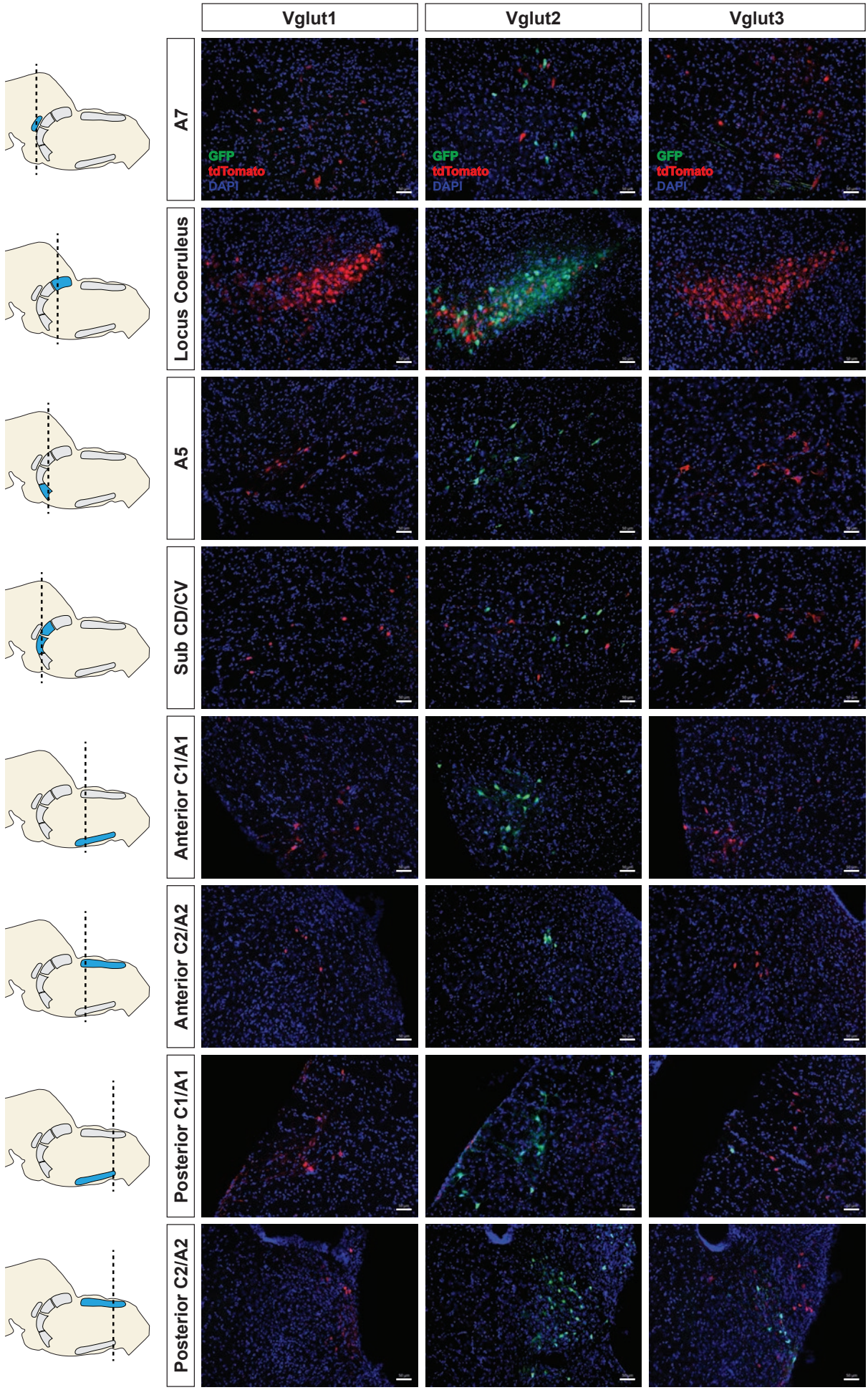

Figure 2

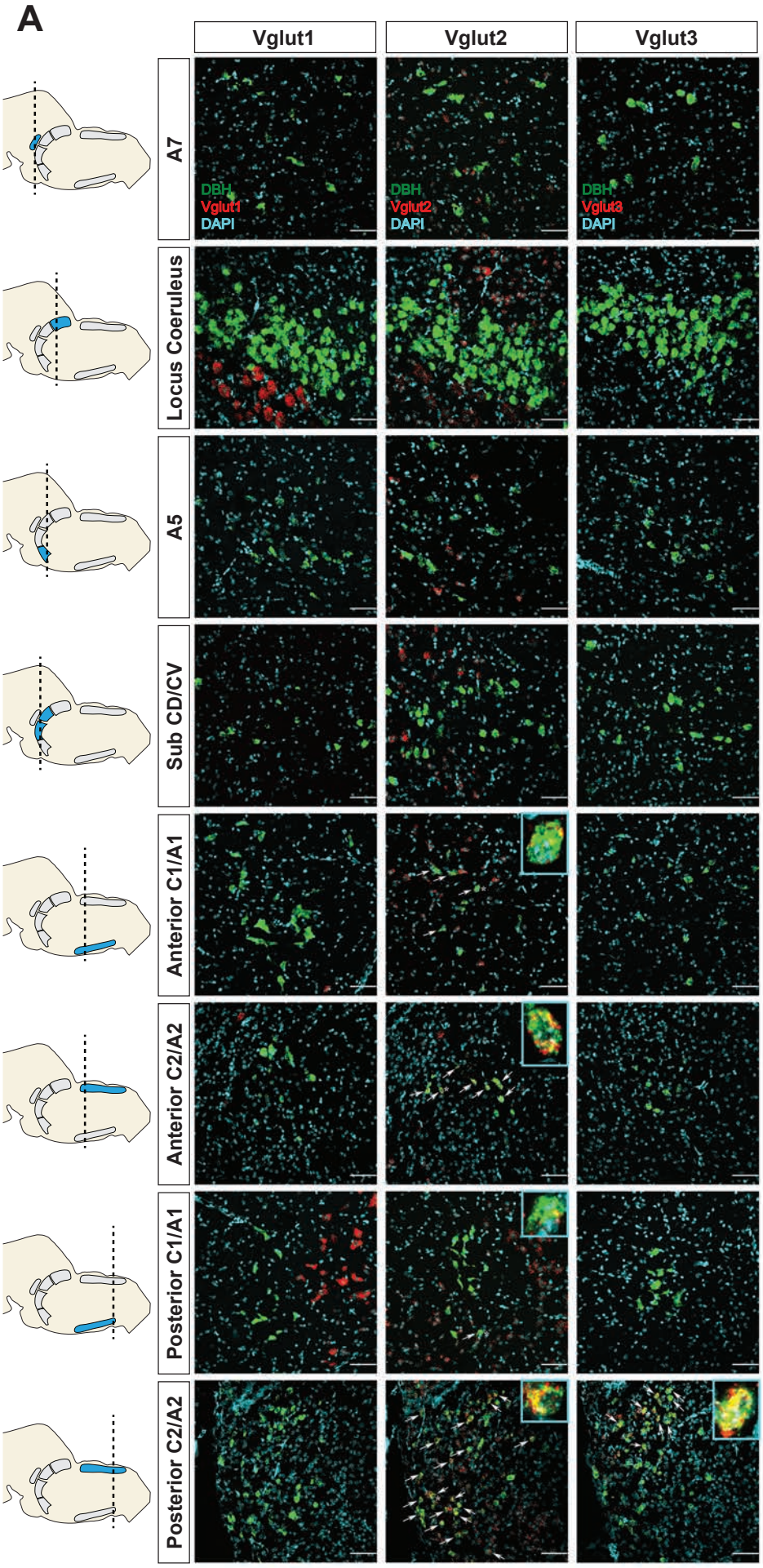
A
Vglut1
Vglut2
Vglut3
A7
Locus Coeruleus
A5
Sub CD/CV
Anterior C1/A1
Anterior C2/A2
Posterior C1/A1
Posterior C2/A2
DBH
Vglut1
DAPI
DBH
Vglut2
DAPI
DBH
Vglut3
DAPI

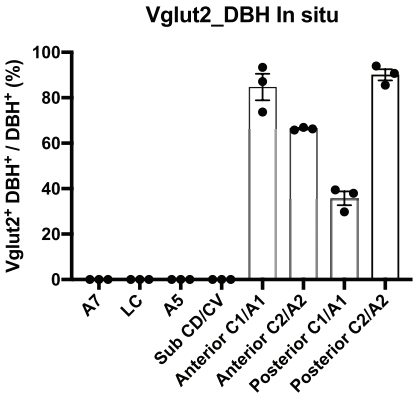
B
Vglut2_DBH In situ
Vglut2+ DBH+ / DBH+ (%)
100
80
60
40
20
0
A7
LC
A5
Sub CD/CV
Anterior C1/A1
Anterior C2/A2
Posterior C1/A1
Posterior C2/A2

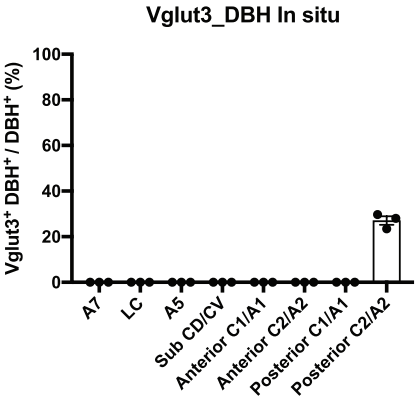
C
Vglut3_DBH In situ
Vglut3+ DBH+ / DBH+ (%)
100
80
60
40
20
0
A7
LC
A5
Sub CD/CV
Anterior C1/A1
Anterior C2/A2
Posterior C1/A1
Posterior C2/A2

Figure 3

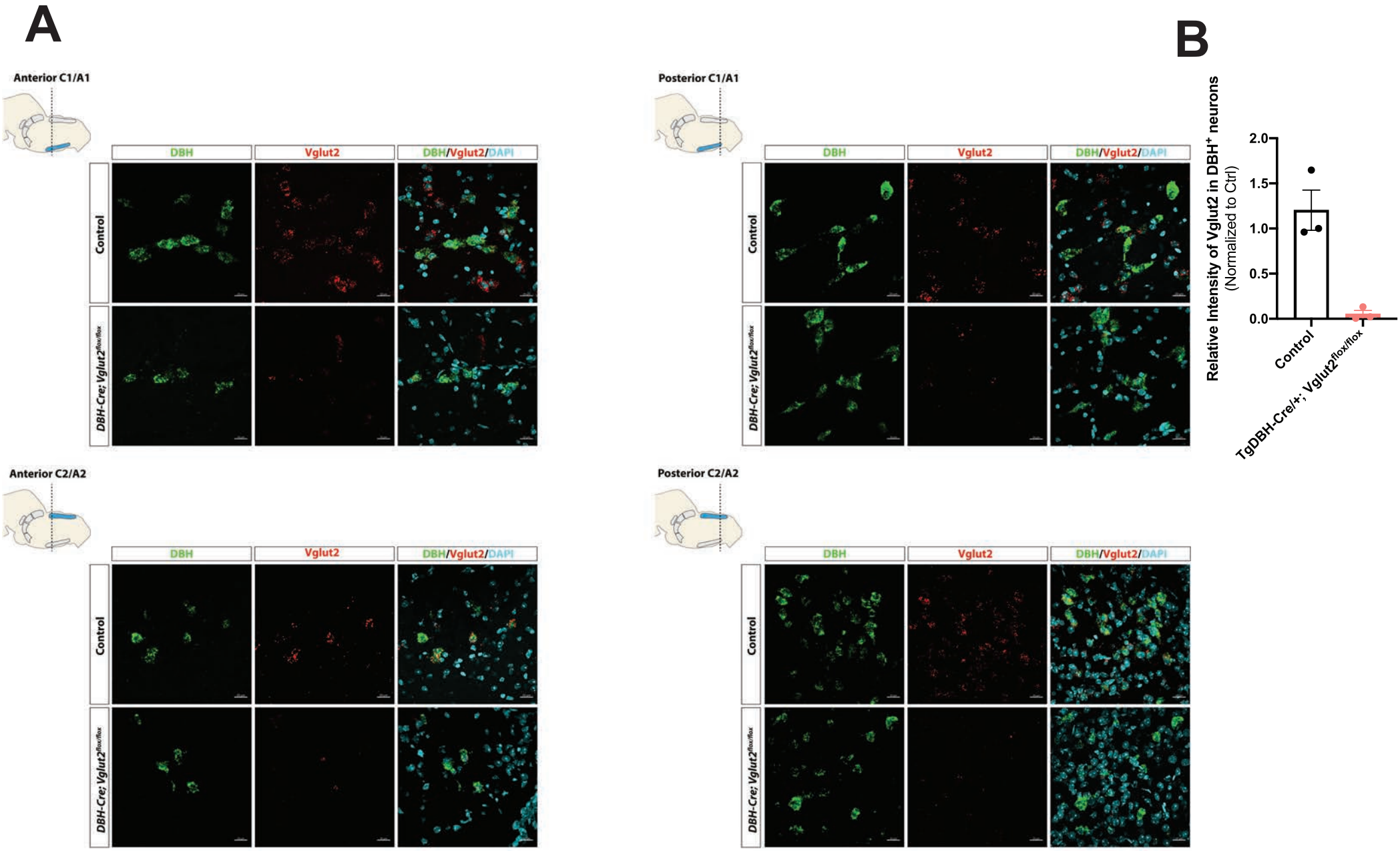
A
Anterior C1/A1
Posterior C1/A1
Anterior C2/A2
Posterior C2/A2
DBH
Vglut2
DBH/Vglut2/DAPI
Control
DBH-Cre; Vglut2flox/flox
B
Relative Intensity of Vglut2 in DBH+ neurons
(Normalized to Ctrl)
2.0
1.5
1.0
0.5
0.0
Control
TgDBH-Cre/+; Vglut2flox/flox

Figure 4

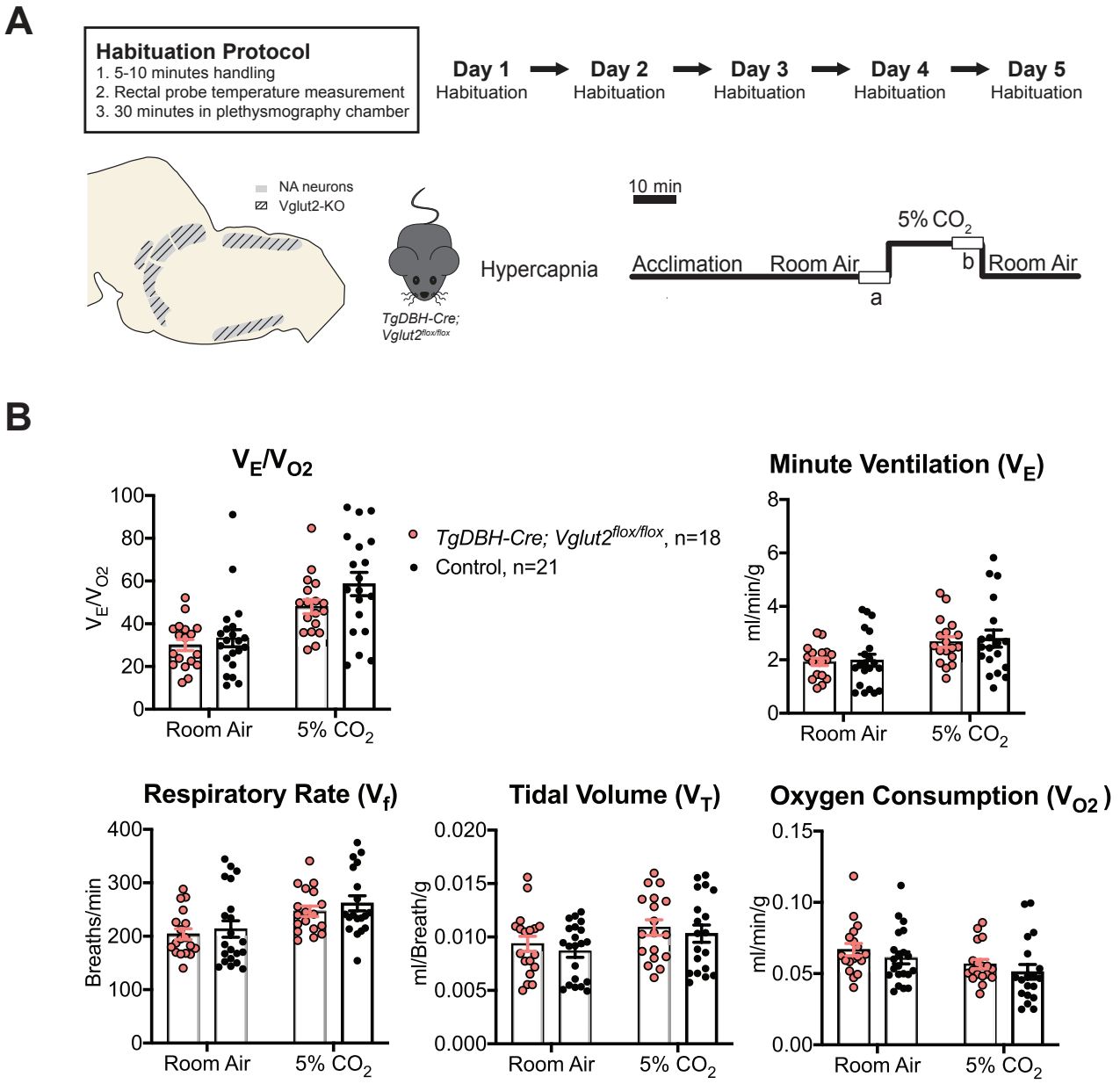
A
Habituation Protocol
1. 5-10 minutes handling
2. Rectal probe temperature measurement
3. 30 minutes in plethysmography chamber
Day 1 Habituation
Day 2 Habituation
Day 3 Habituation
Day 4 Habituation
Day 5 Habituation
NA neurons
Vglut2-KO
TgDBH-Cre; Vglut2flox/flox
Hypercapnia
10 min
5% CO2
Acclimation
Room Air
a
b
Room Air
B
VE/VO2
TgDBH-Cre; Vglut2flox/flox, n=18
Control, n=21
Minute Ventilation (VE)
ml/min/g
Room Air
5% CO2
Respiratory Rate (Vf)
Breaths/min
Tidal Volume (VT)
ml/Breath/g
Oxygen Consumption (VO2)
ml/min/g

Figure 5

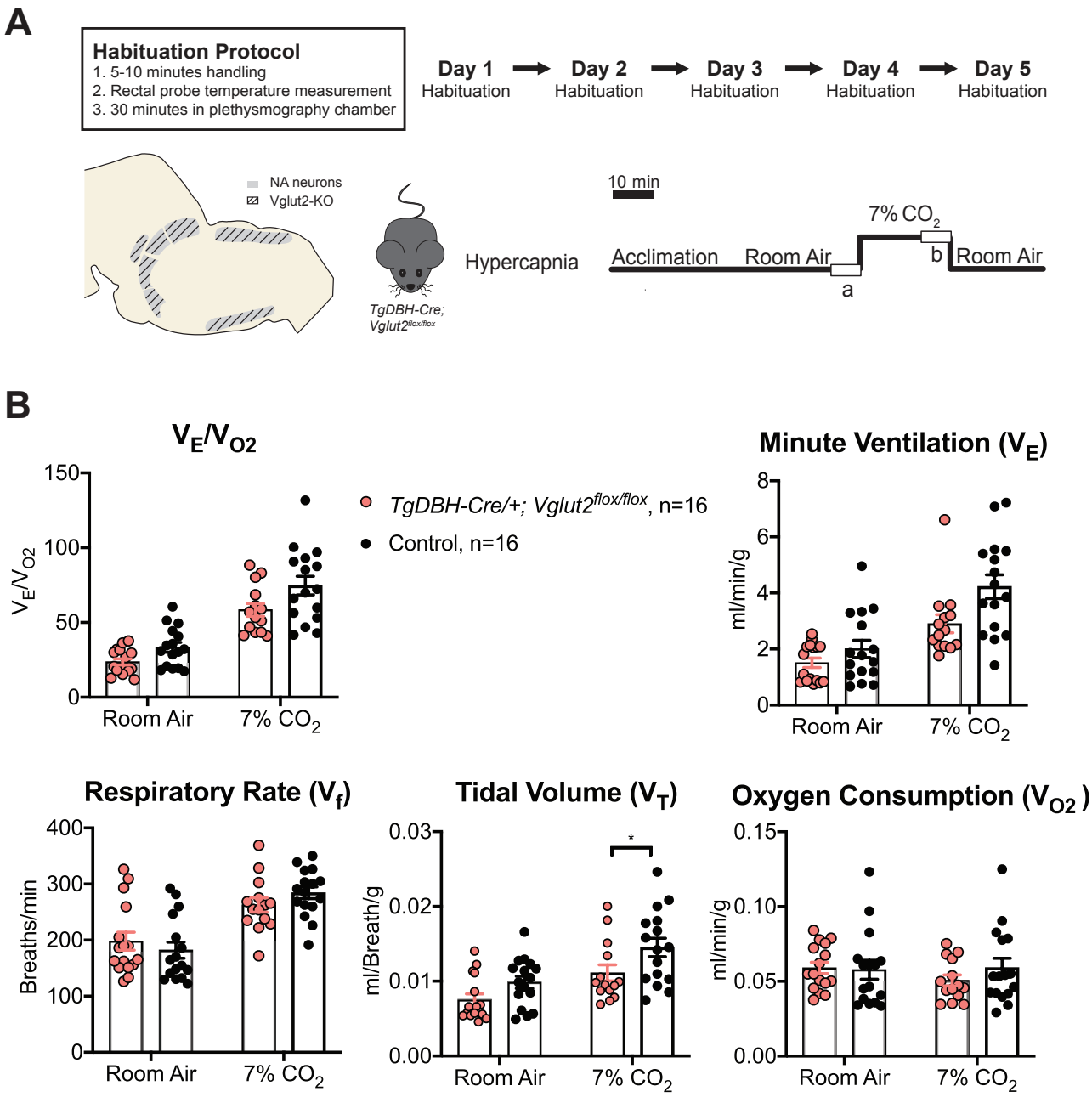
A
Habituation Protocol
1. 5-10 minutes handling
2. Rectal probe temperature measurement
3. 30 minutes in plethysmography chamber
Day 1 Habituation
Day 2 Habituation
Day 3 Habituation
Day 4 Habituation
Day 5 Habituation
NA neurons
Vglut2-KO
TgDBH-Cre; Vglut2flox/flox
Hypercapnia
10 min
Acclimation
Room Air
7% CO2
a
b
Room Air
B
VE/VO2
TgDBH-Cre/+; Vglut2flox/flox, n=16
Control, n=16
Minute Ventilation (VE)
ml/min/g
Room Air
7% CO2
Respiratory Rate (Vf)
Breaths/min
Tidal Volume (VT)
ml/Breath/g
*
Oxygen Consumption (VO2)
ml/min/g

Figure 6

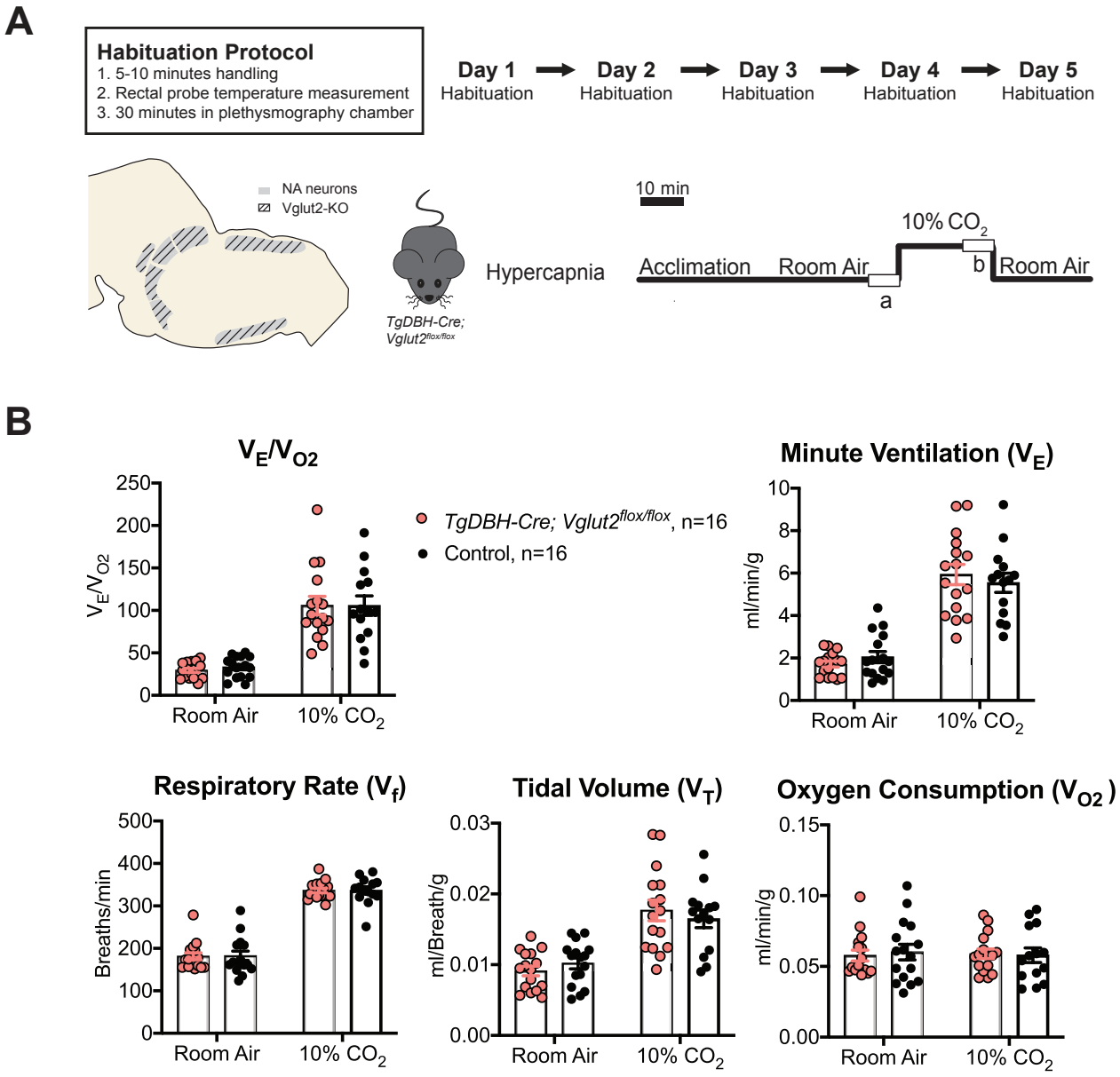
A
Habituation Protocol
1. 5-10 minutes handling
2. Rectal probe temperature measurement
3. 30 minutes in plethysmography chamber
Day 1 Habituation
Day 2 Habituation
Day 3 Habituation
Day 4 Habituation
Day 5 Habituation
NA neurons
Vglut2-KO
TgDBH-Cre; Vglut2flox/flox
Hypercapnia
10 min
10% CO2
Acclimation
Room Air
a
b
Room Air
B
VE/VO2
TgDBH-Cre; Vglut2flox/flox, n=16
Control, n=16
Minute Ventilation (VE)
ml/min/g
Respiratory Rate (Vf)
Breaths/min
Tidal Volume (VT)
ml/Breath/g
Oxygen Consumption (VO2)
ml/min/g
Room Air
10% CO2

Figure 7

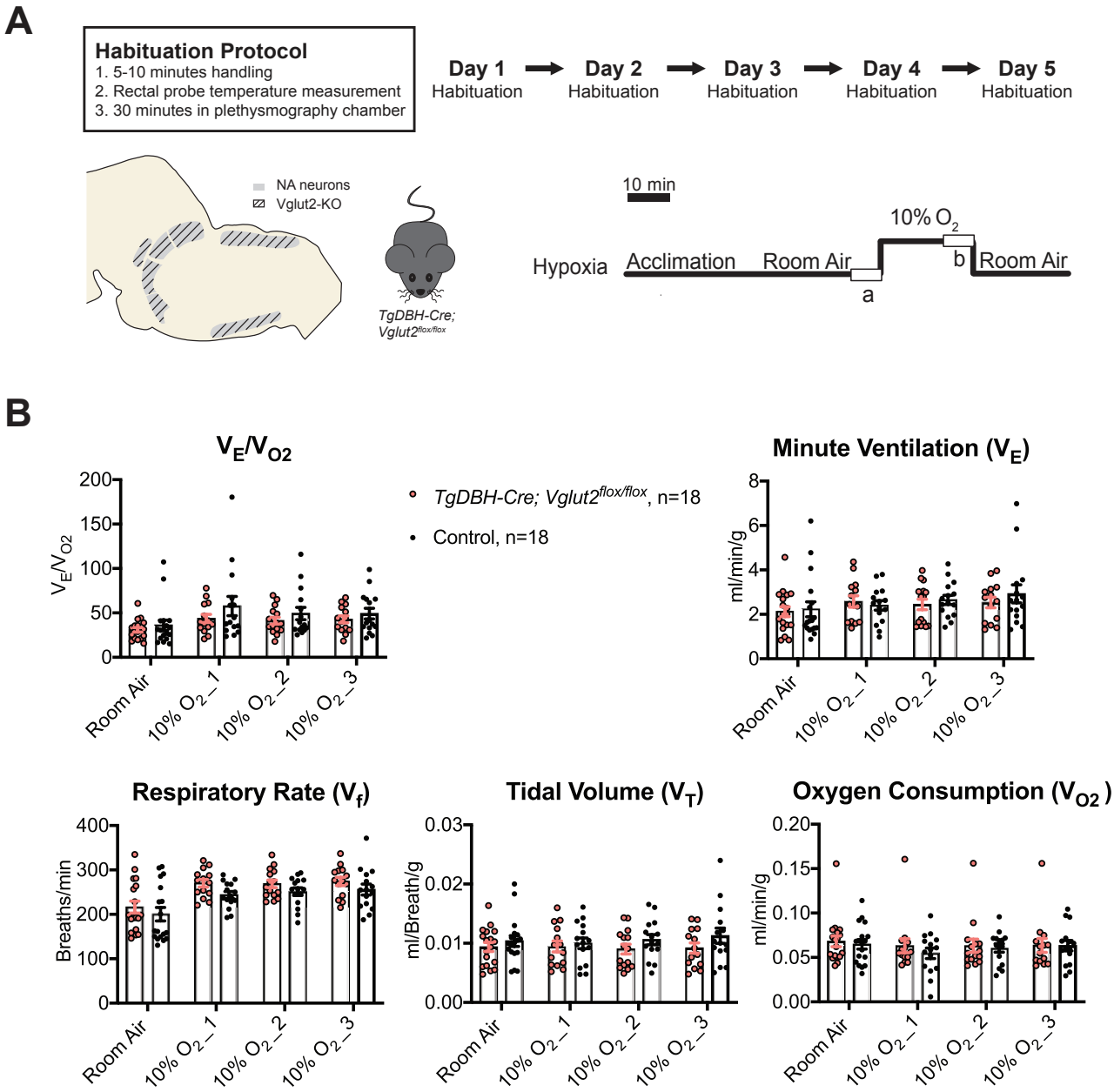
A
Habituation Protocol
1. 5-10 minutes handling
2. Rectal probe temperature measurement
3. 30 minutes in plethysmography chamber
Day 1 Habituation
Day 2 Habituation
Day 3 Habituation
Day 4 Habituation
Day 5 Habituation
NA neurons
Vglut2-KO
TgDBH-Cre; Vglut2flox/flox
10 min
Hypoxia
Acclimation
Room Air
10% O2
a
b
Room Air
B
VE/VO2
TgDBH-Cre; Vglut2flox/flox, n=18
Control, n=18
Minute Ventilation (VE)
ml/min/g
Room Air
10% O2_1
10% O2_2
10% O2_3
Respiratory Rate (Vf)
Breaths/min
Tidal Volume (VT)
ml/Breath/g
Oxygen Consumption (VO2)
ml/min/g

Figure 2 supplement 1

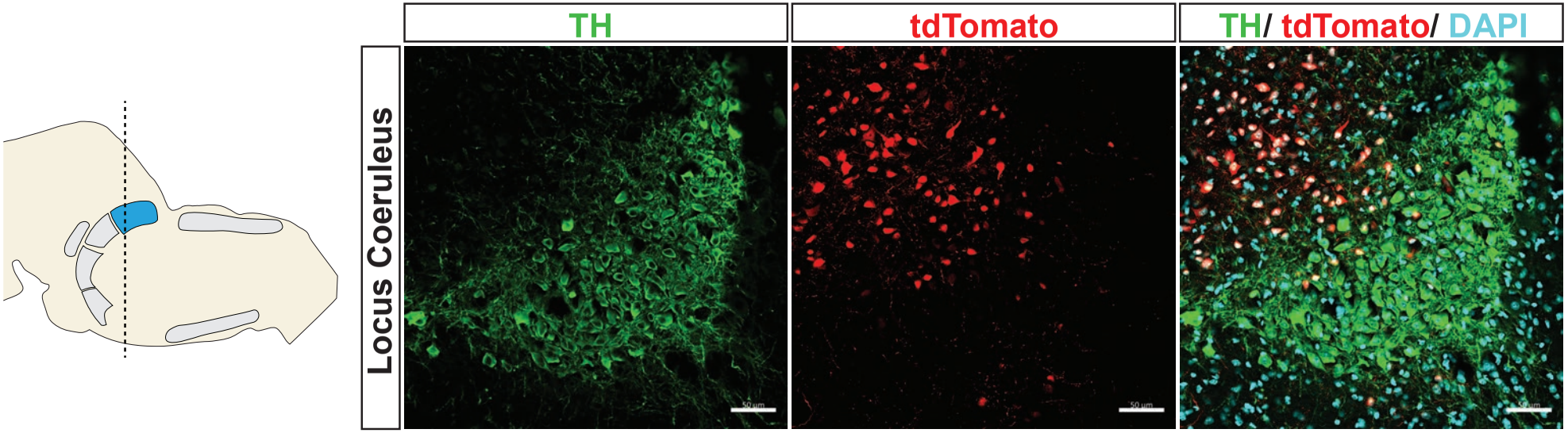

Table 1. Respiratory and metabolic values under room air conditions and the statistical tests

	TgDBH-Cre/+; Vglut2$^{flox/flox}$ **Mean ± SEM**	**Control Mean ± SEM**	***TgDBH-Cre/+; Vglut2$^{flox/flox}$*** **vs Control linear mixed-effects regression model**
V_E/V_{O2}	30.01 ± 2.58	33.22 ± 3.97	P = 0.98
V_f	204.08 ± 10.04	213.58 ± 15.36	P = 0.98
V_T	0.009 ± 0.0007	0.009 ± 0.0006	P = 0.88
V_E	1.93 ± 0.14	1.98 ± 0.22	P = 0.995
V_{O2}	0.067 ± 0.004	0.061 ± 0.004	P = 0.78

Table 2. Respiratory and metabolic values under 5% CO_2 conditions and the statistical tests

	TgDBH-Cre/+; Vglut2$^{flox/flox}$ **Mean ± SEM**	**Control Mean ± SEM**	***TgDBH-Cre/+; Vglut2$^{flox/flox}$*** **vs Control linear mixed-effects regression model**
V_E/V_{O2}	47.99 ± 3.28	58.60 ± 5.44	P = 0.33
V_f	246.72 ± 9.78	261.66 ± 14.00	P = 0.24
V_T	0.011 ± 0.0007	0.010 ± 0.0008	P = 0.81
V_E	2.67 ± 0.20	2.80 ± 0.32	P = 0.98
V_{O2}	0.057 ± 0.003	0.051 ± 0.005	P = 0.42

Table 3. Respiratory and metabolic values under 7% CO_2 conditions and the statistical tests

	TgDBH-Cre/+; Vglut2$^{flox/flox}$ **Mean ± SEM**	**Control Mean ± SEM**	***TgDBH-Cre/+; Vglut2$^{flox/flox}$*** **vs Control linear mixed-effects regression model**
V_E/V_{O2}	58.48 ± 4.29	74.70 ± 6.22	P = 0.23
V_f	262.69 ± 12.82	284.44 ± 10.59	P = 0.98
V_T	0.011 ± 0.0011	0.015 ± 0.0012	P = 0.023*
V_E	2.90 ± 0.32	4.23 ± 0.43	P = 0.16
V_{O2}	0.051 ± 0.004	0.059 ± 0.006	P = 0.64

Table 4. Respiratory and metabolic values under 10% CO_2 conditions and the statistical tests

	TgDBH-Cre/+; Vglut2$^{flox/flox}$ **Mean ± SEM**	**Control Mean ± SEM**	***TgDBH-Cre/+; Vglut2$^{flox/flox}$*** **vs Control linear mixed-effects regression model**
V_E/V_{O2}	105.77 ± 10.80	105.69 ± 11.51	P = 0.9996
V_f	336.31 ± 5.26	336.38 ± 8.52	P = 0.9997
V_T	0.018 ± 0.0015	0.016 ± 0.0012	P = 0.98
V_E	5.94 ± 0.48	5.54 ± 0.45	P = 0.9996
V_{O2}	0.059 ± 0.003	0.058 ± 0.005	P = 0.9999999

Table 5. Respiratory and metabolic values under 10% O_2 conditions and the statistical tests

	TgDBH-Cre/+; Vglut2$^{flox/flox}$ Mean ± SEM	Control Mean ± SEM	Linear mixed-effects regression model	*TgDBH-Cre/+; Vglut2$^{flox/flox}$* Mean ± SEM	Control Mean ± SEM	Linear mixed-effects regression model	*TgDBH-Cre/+; Vglut2$^{flox/flox}$* Mean ± SEM	Control Mean ± SEM	Linear mixed-effects regression model
	10% O_2_1			**10% O_2_2**			**10% O_2_3**		
V_E/V_{O2}	43.79 ± 4.57	57.75 ± 10.88	P = 0.99	41.30 ± 3.85	49.36 ± 6.93	P = 0.99	42.82 ± 3.97	49.19 ± 6.02	P = 0.99
V_f	269.71 ± 8.49	243.89 ± 7.64	P = 0.67	268.38 ± 8.40	251.15 ± 8.67	P = 0.83	273.96 ± 9.31	255.84 ± 12.19	P = 0.80
V_T	0.009 ± 0.0009	0.010 ± 0.0009	P = 0.89	0.009 ± 0.0008	0.011 ± 0.0009	P = 0.85	0.009 ± 0.0009	0.011 ± 0.0013	P = 0.64
V_E	2.58 ± 0.25	2.40 ± 0.21	P = 0.999998	2.45 ± 0.24	2.65 ± 0.21	P = 0.9998	2.53 ± 0.24	2.92 ± 0.41	P = 0.998
V_{O2}	0.063 ± 0.008	0.055 ± 0.006	P = 0.995	0.063 ± 0.007	0.061 ± 0.005	P = 0.9998	0.064 ± 0.008	0.063 ± 0.006	P = 0.99999999

Supplemental table 1. Vglut2$^+$ innervations from central noradrenergic neurons to the brain nuclei important in breathing control

Vglut2$^+$ noradrenergic nuclei	Downstream target of Vglut2$^+$ NA neurons	The role of the downstream target in breathing control	Reference
C1	preBötzinger complex	Generate inspiratory rhythm	Malheiros-Lima et al. (2018)
	parafacial region (pFRG)	Regulate active expiration during chemosensory stimulation	Malheiros-Lima et al. (2020)
	Locus Coeruleus (LC)	Chemosensitive, regulate chemosensation	Abbott et al. (2013); Holloway et al. (2013)
	A5	Inhibitory drive for chemosensation and respiratory rhythm	Abbott et al. (2013); Malheiros-Lima et al. (2022)
	A1, A2	Modulate chemosensation, stabilize respiratory rhythm	Abbott et al. (2013); Holloway et al. (2013)
	Lateral parabrachial nucleus (PBN)	Regulate chemosensation and arousal	Abbott et al. (2013)
	Medullary raphe	Regulate chemosensation and expiration	Abbott et al. (2013)
	Nucleus of the solitary tract (NTS)	Receive input from the carotid bodies (a key center for O_2 chemosensation) and other cardiopulmonary afferents	Abbott et al. (2013)
	Dorsal motor nucleus of the vagus	Control respiration rate, regulate airway tone and defense	Abbott et al. (2013)
	Dorsomedial hypothalamus (DMH) lateral hypothalamic area (LHA)	Modulate baseline respiration, chemosensation, arousal	Abbott et al. (2013)
	Paraventricular thalamic nucleus (PVT)	Regulate arousal	Abbott et al. (2013)
	Paraventricular nucleus (PVN)	Modulate baseline respiration, respiratory response to hypoxia	Abbott et al. (2013)
Locus Coeruleus (LC)	Lateral parabrachial nucleus	Regulate chemosensation and arousal	Yang et al. (2021)